



## Transport slopes, sediment cover, and bedrock channel incision in the Henry Mountains, Utah

Joel P. L. Johnson,<sup>1</sup> Kelin X. Whipple,<sup>2</sup> Leonard S. Sklar,<sup>3</sup> and Thomas C. Hanks<sup>4</sup>

Received 4 July 2007; revised 21 January 2009; accepted 26 February 2009; published 5 May 2009.

[1] Field data from channels in the Henry Mountains of Utah demonstrate that abundant coarse sediment can inhibit fluvial incision into bedrock by armoring channel beds (the cover effect). We compare several small channels that share tributary junctions and have incised into the same sedimentary bedrock unit (Navajo Sandstone) but contain differing amounts of coarse diorite clasts owing to the spatial distribution of localized sediment sources. Bedrock channels that contain abundant clasts (diorite-rich) have steeper longitudinal slopes than tributaries of these channels with smaller drainage areas and less sediment (diorite-poor). The diorite-poor tributaries have incised more deeply to lower average slopes and have more reach-scale slope variability, which may reflect bedrock properties, longitudinal sediment sorting, and incision at lower sediment supply. Diorite-rich channels have less bedrock exposed and smoother longitudinal profiles than diorite-poor channels. We find that (1) coarse sediment can mantle bedrock channel beds and reduce the efficiency of incision, validating the hypothesized cover effect in fluvial incision models; (2) the channel slope needed to transport the sediment load can be larger than that needed to erode bedrock, suggesting that the slope of incising bedrock channels can become adjusted to the sediment load; (3) when abundant sediment is available, transport capacity rather than thresholds of motion can be dominant in setting bedrock channel slope; and (4) cover effects can be important even when moderate amounts of bedrock are exposed in channel beds.

**Citation:** Johnson, J. P. L., K. X. Whipple, L. S. Sklar, and T. C. Hanks (2009), Transport slopes, sediment cover, and bedrock channel incision in the Henry Mountains, Utah, *J. Geophys. Res.*, 114, F02014, doi:10.1029/2007JF000862.

### 1. Statement of the Problem

[2] Channels are conduits for the transport of both water and sediment through eroding landscapes. The sediment load of a river may both enable and inhibit fluvial erosion in incompletely understood ways. Do the slopes of incising channels dominantly adjust to transport sediment, to erode bedrock, or both? How does channel morphology respond to changes in sediment supply, and what are the feedbacks by which channel width, depth and bed roughness in turn influence rates of incision and sediment transport? What level of complexity is needed in bedrock incision models to capture landscape dynamics including hillslope-channel coupling and the sediment flux to the channel network?

[3] The sediment load supplied to channels from hillslopes represents most of the eroded volume of any given landscape. The fluvial channel network covers only a small fraction of the land area, and the volume of bedrock directly

eroded by fluvial processes will almost always be much smaller than the volume of sediment supplied to and transported through channels. High sediment loads may mantle riverbeds and reduce rates of river incision into bedrock, as has long been inferred [e.g., Gilbert, 1877; Davis, 1889; Hunt, 1953] but only recently modeled quantitatively [e.g., Howard *et al.*, 1994; Howard, 1998; Tucker and Slingerland, 1994; Sklar and Dietrich, 1998, 2004; Turowski *et al.*, 2007c]. Mackin [1948] argued that the longitudinal gradient and morphology (width, depth, roughness) of channels tends to become “delicately adjusted” to an equilibrium in which the ability of flow to transport sediment (transport capacity  $Q_t$ , volume/time) equals the sediment flux ( $Q_s$ , volume/time) supplied to the channel. Mackin [1948] suggested that not only entirely alluvial channels but also rivers exhibiting long-term incision into bedrock can equilibrate such that  $Q_s = Q_t$ . Sklar and Dietrich [1998, 2004, 2006] and Whipple and Tucker [2002] have similarly shown that many sediment flux-dependent fluvial incision models predict the occurrence of bedrock rivers which are graded to transport the bed load supply but still actively incise through bedrock. We explore whether such channels actually exist in nature.

[4] In this contribution we use field observations to evaluate proposed models for the role of sediment cover in fluvial incision, to better understand channels with beds that are largely blanketed with alluvium but that incise into bedrock on millennial time scales. We exploit a field setting

<sup>1</sup>Jackson School of Geosciences, University of Texas at Austin, Austin, Texas, USA.

<sup>2</sup>School of Earth and Space Exploration, Arizona State University, Tempe, Arizona, USA.

<sup>3</sup>Department of Geosciences, San Francisco State University, San Francisco, California, USA.

<sup>4</sup>U.S. Geological Survey, Menlo Park, California, USA.

where channels experiencing a common base level fall history, but receiving variable amounts of coarse bed load, can be directly compared to determine how bedrock incision and channel slope have been influenced by bed load supply.

## 2. Definitions and Cover Models

[5] *Howard* [1998] defined mixed bedrock–alluvial channels as having bedrock exposed over “say 5% to 60% of total bed area” and having sediment thicknesses less than  $\sim 2\text{--}3$  m, such that large floods can scour through the alluvium and erode bedrock. All of the channels that we discuss have partial sediment cover and are consistent with this definition. They also qualify as bedrock channels following the definition of *Turowski et al.* [2007b] that a bedrock channel is one which “cannot substantially widen, lower, or shift its bed without eroding bedrock.” Bedrock channels are in practice classified as such if bedrock is exposed in the riverbed and banks [e.g., *Howard et al.*, 1994; *Montgomery et al.*, 1996; *Howard*, 1998; *Whipple*, 2004; *Turowski et al.*, 2007b].

[6] In an idealized steady state landscape, the local erosion rate along all channels is adjusted to equal the long-term base level lowering rate imposed at some location downstream. Channel slope, morphology and bed state (percent alluvial cover, grain size distribution, bed forms) adjust in concert to both match this incision rate and to transport the sediment load supplied to the channel. Away from steady state this adjustment will be incomplete, but channels will progress toward a steady state configuration.

[7] Following *Sklar and Dietrich* [2004], we define the efficiency of erosion as the ratio of the stream power (rate of energy dissipation) of the flow that directly contributes to eroding bedrock to the total stream power expended by the flow. If we compare two channels at the same discharge, width, slope, and bedrock strength away from steady state, the more rapidly incising channel has more efficient erosion (perhaps owing to differences in bed cover). Comparing two channels of the same discharge and width in a steady state eroding landscape, the steeper channel indicates less efficient incision, because the lower slope channel would have lower stream power but the same incision rate (at steady state, by definition). Framing our arguments in terms of erosional efficiency allows us to interpret both rates and patterns of bedrock incision over a range of equilibrium to disequilibrium conditions. We later interpret differences in erosional efficiency between channels on the basis of reach slopes, argue that observed slope differences are inconsistent with nonsteady state effects alone, and interpret how differences in sediment load influence the efficiency of river incision into bedrock.

### 2.1. Slope, Supply, and Sediment Load–Dominated Bedrock Channels

[8] At steady state, *Sklar and Dietrich* [2006] suggest that sediment and bedrock controls on incision can be expressed as components of the total channel longitudinal slope:

$$S = S_{cr} + \Delta S_{qs} + \Delta S_e \quad (1)$$

where  $S_{cr}$  is the slope necessary to just exceed the sediment threshold of motion,  $\Delta S_{qs}$  is the additional slope needed to

transport the sediment load supplied from upstream, and  $\Delta S_e$  is the additional slope that contributes directly to bedrock erosion at a rate equal to the base level lowering rate. During transient incision, the difference between  $S_{cr} + \Delta S_{qs}$  and  $S$  reflects not only  $\Delta S_e$  but also previous conditions. Using the saltation-abrasion model, *Sklar and Dietrich* [2006] found that  $\Delta S_e \ll S$  over most parameter space (discharge, sediment size, sediment flux, rock strength, uplift rate), meaning that only a slight increase in slope above that needed to transport the sediment load ( $S_{cr} + \Delta S_{qs}$ ) may be sufficient to erode at geomorphically common rates. The saltation-abrasion model predicts that inherent bedrock properties (e.g., strength, erodibility) are secondary to sediment supply in setting channel slope, except for the most durable rocks and the most rapid uplift rates.

[9] It is therefore plausible that the slope and morphology of an incising bedrock channel may primarily be adjusted to transport the sediment load. We propose the term “sediment load–dominated bedrock channels” to describe this class of channels, defined as those where  $S_{cr} + \Delta S_{qs} \gg \Delta S_e$ . This condition implies that sediment flux and sediment transport capacity are roughly equal (i.e.,  $Q_s/Q_t \sim 1$ ). Sediment load–dominated channels have equivalently been referred to as “transport-limited” [e.g., *Whipple and Tucker*, 2002; *Brocard and van der Beek*, 2006; *Jansen*, 2006; *Johnson and Whipple*, 2007]. In this usage, the quantity that is being “limited” is vertical lowering (erosion) along the channel, as a result of the sediment load. However, “transport-limited” has also been used to mean that the sediment flux is limited by the transport capacity, i.e.,  $Q_s/Q_t \geq 1$  [e.g., *Davy and Crave*, 2000; *Lague et al.*, 2003]. In this usage the quantity being “limited” is the sediment flux, and any channel in which  $Q_t$  exceeds  $Q_s$  even slightly would therefore not be transport-limited. Owing to this definitional ambiguity, we have not used the “transport-limited” terminology in this paper.

### 2.2. Model Comparisons and the Cover Effect

[10] A range of bedrock incision models have been proposed, from some that do not explicitly consider the sediment load to some in which the dynamic behavior of incising bedrock channels is identical to that of alluvial rivers [e.g., *Willgoose et al.*, 1991]. We next categorize several models on the basis of their treatment of sediment load and cover effects. First, the shear stress (or stream power) incision model does not include cover effects or any explicit dependence on sediment supply, but rather holds that incision rate is a power law function of shear stress (or stream power) exerted on the channel bed by the flow of water [e.g., *Howard and Kerby*, 1983; *Whipple and Tucker*, 1999, 2002; *Stock and Montgomery*, 1999; *Lave and Avouac*, 2001; *Lague et al.*, 2005]. In a second variant of this model, the shear stress incision rule can be coupled to a model for predicting alluvial channel profiles: shear stress erosion model for  $Q_s < Q_t$ , alluvial channel for  $Q_s > Q_t$  [e.g., *Howard et al.*, 1994; *Tucker and Slingerland*, 1994; *Whipple and Tucker*, 2002]. This forms the simplest category of cover models, in which the cover effect is all or nothing: sediment only inhibits incision once  $Q_s > Q_t$  and so bedrock incision is not influenced by sediment until cover is complete. *Hancock and Anderson* [2002] present a similar cover

model in which limited bedrock erosion can occur under a thin veneer of alluvial cover. A third category includes cover models in which bed cover gradually increases, and erosional efficiency decreases, as  $Q_s$  approaches  $Q_t$ . In these models, erosional efficiency decreases with increasing sediment supply even when bedrock is partially exposed on the bed and  $Q_s$  is well under  $Q_t$  [Beaumont *et al.*, 1992; Sklar and Dietrich, 1998, 2004; Turowski *et al.*, 2007c]. Later, we qualitatively evaluate these three categories of cover models on the basis of field data.

[11] The presence or absence of slope breaks at lithologic contacts is a potentially diagnostic difference between bedrock incision models that can be observed in the field. Whipple and Tucker [2002] calculated channel profiles using different incision models, and found that the slopes of sediment load–dominated bedrock rivers exhibit smooth transitions, or no changes at all, at lithologic contacts or where crossing active structures. As a channel incises down, feedbacks dictate that the slope remains steep enough to transport its sediment supply. In a sediment load–dominated bedrock channel, local slopes are controlled by the integrated sediment flux from upstream and are insensitive to local substrate properties.

[12] In contrast, models in which erosional efficiency depends strongly on local substrate properties, including the shear stress erosion model, predict sharp breaks in slope at lithologic transitions. In addition to the cover effect (in which erosional efficiency decreases with increasing sediment flux), the saltation-abrasion model [Sklar and Dietrich, 1998, 2004] also includes a “tools effect” in which erosional efficiency increases with sediment flux. A physical mechanism for the tools effect is that higher sediment flux increases the rate of bed load impacts on the bedrock bed. The saltation-abrasion model predicts that channels incising at low sediment supply (i.e., where tools effects are dominant) will have variations in bedrock properties expressed in the channel profile. Abundant bedrock will be exposed on the bed and the local incision rate will depend directly on rock strength.

### 2.3. Field Tests

[13] Although both tools and cover effects have been demonstrated in laboratory experiments [e.g., Sklar and Dietrich, 2001; Johnson and Whipple, 2007; Finnegan *et al.*, 2007; Johnson, 2007; Chatanantavet and Parker, 2008], field-based tests remain limited. Brocard and van der Beek [2006] and Jansen [2006] inferred sediment load–dominated channel incision on the basis of longitudinal channel profiles, mapped bedrock lithology and field observations in the French Alps and Australia, respectively. Turowski *et al.* [2007a] observed extensive sediment cover following a large flood in a natural bedrock channel in Taiwan, and inferred that the distribution of bedrock erosion was consistent with cover effects. Cowie *et al.* [2008] found field evidence for both tools and cover effects on long-term channel incision on the basis of transient basin adjustments in response to tectonic forcing. Additional studies that evaluate bedrock incision model formulations using field data include those of Stock and Montgomery [1999], Lave and Avouac [2001], van der Beek and Bishop [2003], Tomkin *et al.* [2003], and Crosby *et al.* [2007].

[14] Channels in the Henry Mountains of Utah provide an excellent opportunity to isolate the influence of sediment supply on bedrock channel incision. In section 4, we present field survey techniques used to quantify differences in local morphology, bedrock exposure and sediment size distribution between channels. In the Results section, we first present a regional digital elevation model (DEM) and remote sensing analysis of channel longitudinal profiles, bedrock lithology and sediment availability. We then compare field surveys of three channels in the same drainage network that have different coarse sediment loads and have incised to different channel slopes. In section 6, we argue that the slopes of the incising channels with abundant sediment supply are adjusted to transport their coarse sediment loads. We find that some simple cover models are inconsistent with our field observations, and we discuss how bed roughness and channel morphology may evolve as sediment supply is reduced.

### 3. Henry Mountains, Utah

[15] The Henry Mountains are useful for isolating sedimentary and lithologic controls on river incision into rock because (1) channels incise through the same sedimentary rock units, which have a range of strengths and resistances to weathering and (2) the coarse sediment load (amount, hardness, size distribution) varies between channels. The five Henry Mountain peaks formed as a result of Tertiary igneous intrusions of diorite that form the cores of the mountains (Figure 1) [Gilbert, 1877; Hunt, 1953; Jackson and Pollard, 1990]. Mesozoic sedimentary units surround the central peaks. Near intrusions, sedimentary beds are often broadly warped but show minimal deformation. Away from intrusions, beds are nearly horizontal. Exposures of diorite bedrock and colluvium are found near the mountain peaks. Abundant coarse diorite sediment is supplied to the subset of channels whose watersheds include these exposures, as well as from the mobilization of coarse sediment previously stored in fill terraces and on pediments (Figure 1). Channels whose watersheds contain limited diorite sources transport fewer diorite clasts. Some channels have no present-day source for diorite sediment. Bed load is limited in these channels because much of the sediment derived from local lithologies (sandstones, mudstones) is sand. Consequently, channels are supplied with systematically variable amounts of coarse sediment.

[16] Ongoing dissection of the Colorado Plateau in Southeast Utah has been driven by Colorado River incision in its Glen Canyon reach [Hanks *et al.*, 2001; Marchetti and Cerling, 2001; Garvin *et al.*, 2005]. Using cosmogenic exposure age dating of alluvial gravels perched on strath terraces and pediment surfaces near Navajo Mountain, Hanks *et al.* [2001] and Garvin *et al.* [2005] measure incision rates of  $\sim 0.4$  mm a<sup>-1</sup> to  $0.7$  mm a<sup>-1</sup> over the last  $\sim 500$  ka for the Colorado River in Glen Canyon. In the Henry Mountains vicinity, Cook *et al.* [2009] found average incision rates of  $\sim 0.4$  mm a<sup>-1</sup> over the last  $\sim 200$  ka from terrace gravels along Trachyte Creek (Figure 1), more than 20 km upstream from its confluence with the Colorado River. The consistency of measured rates suggests that incision along Trachyte Creek has responded to and may

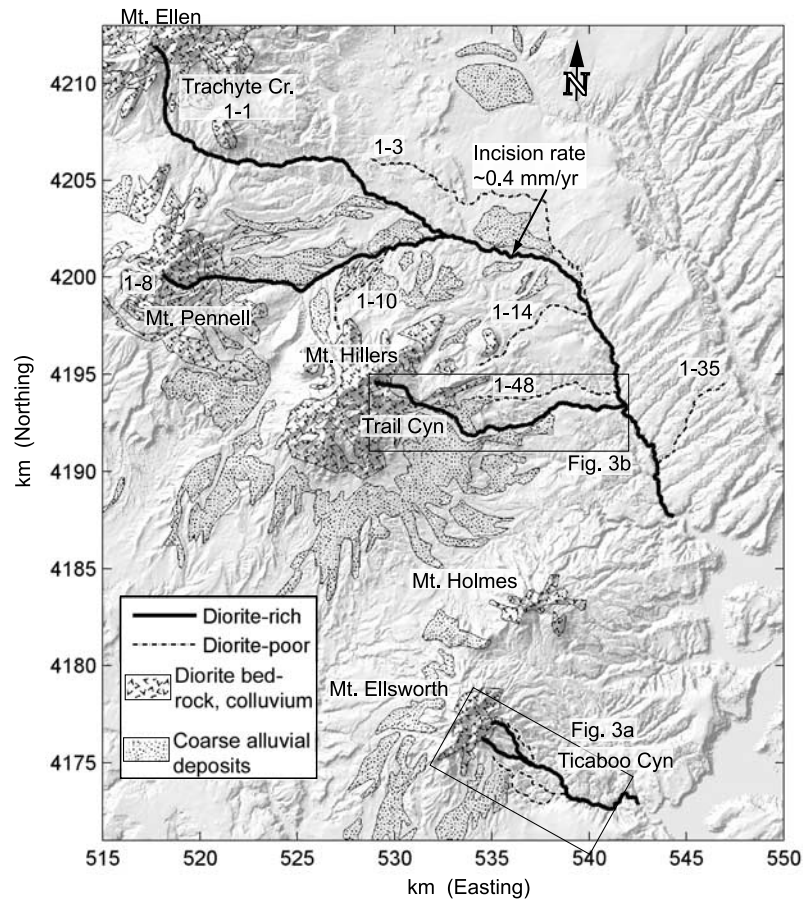


**Figure 1.** The spatial distribution of diorite bedrock, colluvium, and pediment alluvium derived from *Hintze et al.* [2000] is overlain on a shaded relief map of the Henry Mountains, Utah. Some channels contain abundant diorite clasts (diorite-rich), while other channels transport less coarse sediment (diorite-poor). A small but representative subset of profiles with unambiguous diorite sediment classifications is shown. Channel traces are calculated from USGS 10 m digital elevation model (DEMs). Map coordinates are given in the Universal Transverse Mercator Projection (UTM) 12N, Nad27 (zone 12 north, North American datum of 1927); area covered is approximately  $110^{\circ}27'$  to  $110^{\circ}50'W$ ,  $37^{\circ}41'$  to  $38^{\circ}04'N$ . Channel numbers were assigned as part of the regional analysis, with the first number identifying the DEM-derived watershed (e.g., watershed 1 is Trachyte Creek upstream of Lake Powell) and the second identifying the channel within the watershed.

have kept pace with the cutting of Glen Canyon by the Colorado River.

[17] Beyond possibly controlling Colorado River base level, there is no indication of Quaternary tectonic deformation acting within the Henry Mountains or driving differential incision over the relatively small area we study. Therefore, this field site allows us to isolate coarse sediment supply from local tectonics as a control on patterns of channel incision in an eroding landscape. *Cook et al.* [2009] show that incision in our study area remains active at millennial time scales, although incision is also punctuated by intervals of aggradation represented by fill terraces and alluvial treads on strath terraces [*Hunt, 1953; Cook et al., 2009*].

[18] We focused detailed field measurements on channel reaches incised into the Triassic to Jurassic Navajo Sandstone (Jn), an eolian cross-bedded sandstone that is weak on a granular scale but forms large cliffs owing to its lithologic

homogeneity and the wide spacing of joints [e.g., *Schumm and Chorley, 1966*]. The few Navajo Sandstone bedrock clasts produced locally by plucking and rockfall tend to weather rapidly and disaggregate into sand. Above the Navajo Sandstone, the Jurassic Carmel Formation (Jca) is composed of shallow marine siltstones and evaporites with some minor carbonate beds. This unit weathers easily and tends to form gentle hillslopes. Above Jca is the Entrada sandstone (Je), a homogeneous fluvial/eolian sandstone that forms rounded cliffs comparable to the Navajo Sandstone. Our laboratory measurements show that the Navajo Sandstone (tensile strength  $0.25 \pm 0.034$  MPa, 2 standard errors) is at the low end of the range of natural rock strengths measured by *Sklar and Dietrich* [2001], and is nearly 2 orders of magnitude weaker and less abrasion-resistant (measured in a sediment tumbler) than the diorite (tensile strength  $12.9 \pm 0.7$  MPa, 2 standard errors). Tensile strengths of rock cores were measured using the

Brazilian tensile splitting test [Vutukuri *et al.*, 1974; Sklar and Dietrich, 2001].

[19] The arid and rugged Henry Mountains have seen little modification from land use changes and other anthropogenic influences. Cattle and sheep ranching have been attempted for more than a century, but the scarcity of water and vegetation have meant little success, minimizing landscape impact [Kelsey, 1990]. Flow only occurs during flash floods from summer and fall thunderstorms, and from spring snowmelt in channels that drain higher elevations [Johnson *et al.*, 2005]. The channels that we study are not gauged and so we have no direct measures of flow intermittency or magnitudes. However, over several months of field work, we have seen flow (below bankfull) in most channels. A compensating benefit of studying fluvial transport and erosion in dry riverbeds is that the entire channel bottom can be easily observed. A 3-year record of flow and erosion collected in a nearby channel also demonstrates that bed load transport and incision into bedrock are active in the current arid climate [Johnson *et al.*, 2005].

#### 4. Methods

[20] We first conducted a regional analysis of channel profiles. Longitudinal profiles and drainage areas (a proxy for discharge) were calculated from USGS 10 m DEMs, following methods described by Wobus *et al.* [2006]. Profiles were subsampled to approximately extract the original contour crossings from the maps digitized to create the DEMs because interpolation algorithms used in DEM construction introduced stair-step artifacts at contour crossings. In order to preserve local gradient variability along the channels, we did not smooth the profiles.

[21] We selected a subset of channels for detailed field surveys of longitudinal profiles, reach morphology and bed state. Surveying hardware consisted of a GPS, laser rangefinder with a digital inclinometer and compass (Impulse 200/Mapstar), and data logger (a PDA with custom Arcpad scripts). According to the manufacturer, measurement accuracy is  $\pm 0.1$  degrees in inclination and  $\pm 0.3$  degrees in azimuth, and distance resolution is 1 cm. At each survey location we measured the following variables: reach length, slope, bankfull width and depth (using the rangefinder), mean and maximum sediment size (visual estimates), the fractions of bedrock exposed on the channel bed and banks (visual estimates), and the heights of strath and fill terraces relative to the channel bottom (rangefinder). Channels are inherently three-dimensional. To minimize subjectivity in reducing complex local morphology to the above variables, reach endpoint locations were chosen so that the survey would accurately record channel sinuosity as well as changes in local slope, bedrock exposure and bed steps larger than  $\sim 0.5$  m. Surveyed reach distances varied widely, with an average of  $\sim 25$  m.

[22] We measured bankfull widths and depths on the basis of the local channel cross-sectional geometry. Where one or both banks were alluvial, bankfull widths and depths were measured at the slope break between the alluvial bank and floodplain. Where both banks were bedrock, the channel was typically a bedrock-walled slot. Widths but not depths were measured when both walls were vertical to subvertical bedrock. Uncertainties in defining bankfull width and depth

varied with local reach morphology and probably ranged up to  $\pm 20\%$  of individual measured values. The spatial percentages of bedrock exposed in the channel bed and banks ( $100 \times$  area of exposed bedrock/total area) were estimated visually, typically in increments of 10%. One of the criteria for starting a new survey reach was a large change in bedrock exposure, and so values vary widely between reaches. The uncertainty for intermediate bedrock exposure estimates probably also ranged up to  $\pm 20\%$ . However, because there was no measurement uncertainty at 0 or 100% exposure, the overall channel-averaged uncertainties are much lower than  $\pm 20\%$ . In order to minimize user bias, all surveys were conducted by J. Johnson.

[23] In a small subset of channel reaches we measured sediment size distributions by conducting pebble counts, measuring the intermediate diameters of between approximately 50 and 500 clasts. Random walks were followed within predetermined channel reaches [e.g., Leopold, 1970; Wohl *et al.*, 1996]. Pebble count reaches ranged in length from  $\sim 10$  to 50 m, on the basis of local reach slope and morphology. Particles smaller than 3 mm were categorized as “fine” and consisted primarily of sand. The pebble counts were measured by the same two individuals in equal proportions in each reach, removing error due to variability between users in measuring diameters [Wohl *et al.*, 1996]. We also estimated the mean and maximum sediment size in all surveyed reaches, although those measurements are not presented.

[24] The question of whether incision rates are similar between the surveyed channels is important because we interpret differences in erosional efficiency on the basis of present-day channel profiles and morphologies. As noted earlier, incision on the channels we study probably kept pace with the incision rate of the Colorado River [Hanks *et al.*, 2001; Garvin *et al.*, 2005; Cook *et al.*, 2009]. However, we cannot demonstrate that a quasi-equilibrium condition has prevailed over the time scale of channel adjustment. We restrict our analysis to a comparison of channels that are linked by tributary junctions and that grade to the same level, lacking steps or zones of steepening at or near tributary junctions. Under these conditions, incision rates should match in the immediate vicinity of the confluence [Playfair, 1802; Seidl and Dietrich, 1992]. Upstream of the confluence the incision rate of the tributary stream must be greater than or equal to that of the trunk stream. If it were less a steeper reach would develop near the confluence [e.g., Crosby *et al.*, 2007]. The degree of disequilibrium, and how long it can persist, is limited since the trunk stream provides the local base level for the tributary. We conclude that incision rates on the channels with shared confluences are likely similar. At most, incision rates on the smaller tributaries may somewhat exceed the incision rates of the trunk streams. Assuming uniform millennial-scale incision rates is a conservative assumption in our interpretations of the controls on the efficiency of river incision.

#### 5. Results

[25] We first present longitudinal channel profiles from DEM analysis and compare them to interpretations of coarse sediment availability from remote sensing and field observations. Differences in availability of coarse sediment

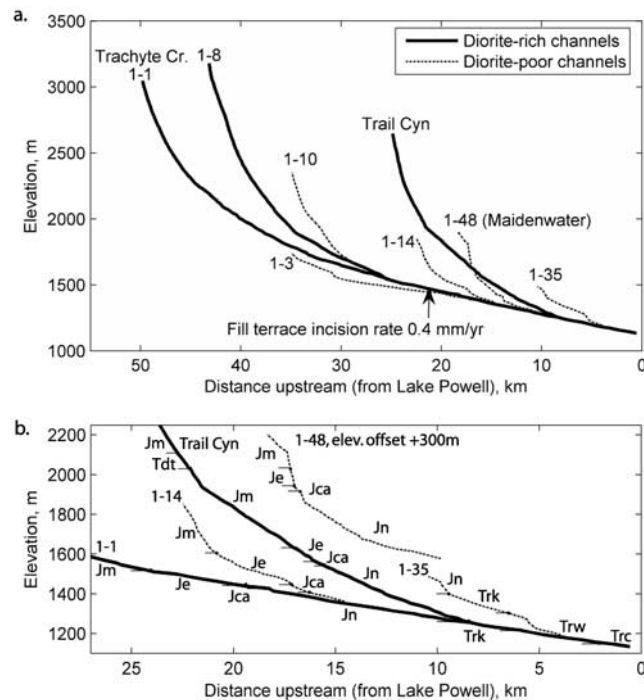


**Figure 2.** DEM Longitudinal profiles for channels in Figure 1. (a) Diorite-rich channels tend to have smoothly concave profiles that start at higher elevations (where the diorite sources are preferentially located), while channels with less coarse sediment have more variable slopes. (b) Contact locations are indicated along a subset of profiles shown in Figure 2a. Slope breaks in diorite-poor channels sometimes, but not always, correspond to contacts between mapped bedrock units. Differences in elevation and unit thickness are due to small and variable regional dips. Trc, Chinle Formation; Trw, Wingate Formation; Trk, Kayenta Formation; Jn, Navajo Sandstone; Jca, Carmel Formation; Je, Entrada Formation; Jm, Summerville and Morrison formations; Tdt, diorite intrusion.

correlate with differences in channel incision and profile smoothness. Results of the DEM analysis guided the selection of channel reaches for detailed field surveys and data analysis, providing field tests of hypotheses on bedrock channel incision.

### 5.1. DEM Profile Analysis

[26] We evaluated the distribution of bedrock lithology and diorite availability on the basis of previous mapping [Hunt, 1953; Hintze and Stokes, 1963; Jackson and Pollard, 1990; Hintze et al., 2000], stereo aerial photography, and Landsat and ASTER multispectral imagery (Figure 1). Lithologic interpretations of 56 channels were compared to DEM profiles, and many of these channels were visited in the field. Channels were classified as either having or not having an abundant supply of coarse diorite sediment (diorite-rich or diorite-poor channels, respectively) from erosion of either bedrock in the headwaters or colluvial and alluvial cover on the mountain flanks and pediments. Diorite-rich channels tend to have smoother and more uniformly concave profiles than diorite-poor channels (Figure 2a). Diorite-rich channels tend to start at higher elevations because diorite sources are most abundant around the mountain peaks. Diorite-poor channels often have slope breaks at lithologic contacts, while the slopes of diorite-rich channels are largely independent of substrate lithology (Figure 2b).

[27] Figures 3a and 4a show Ticaboo Canyon channels that are linked by tributary junctions and are incised into the same bedrock lithologies, primarily Navajo Sandstone (Jn). Slopes just upstream of the main stem confluences are much lower on all three diorite-poor tributaries (3-1, 3-2, 3-5) than on the diorite-rich main stem channels (3-4, 3-6).

[28] Similarly, Figures 2, 3b, and 4b show that the Trail Canyon profile is steeper than Maidenwater Canyon (1-48) and adjacent unnamed tributaries of Trail Canyon (Trib43, 44) near their shared confluences, even though the drainage area of Trail Canyon is much larger. This pattern is surprising because smaller drainage areas usually correspond to higher longitudinal slopes [e.g., Flint, 1974]. Because they share tributary junctions the rate of base level fall has been the same for both main stem and tributary branches, suggesting more efficient incision of the sediment-poor tributaries. Hanging valleys do not occur at the tributary junctions, demonstrating that tributary incision in the vicinity of the confluences has at least kept pace with main stem incision. Steeper reaches are observed along most tributaries, but at even smaller drainage areas well upstream of the confluences of interest. In the Ticaboo Canyon tributaries, field observations of stratigraphic horizons indicate that steep cliffs several kilometers upstream of their main stem confluences occur within the Navajo Sandstone, but close to the underlying contact with the less permeable Kayenta Formation. It is plausible that the lower gradients of the tributaries in part reflect weaker bedrock in

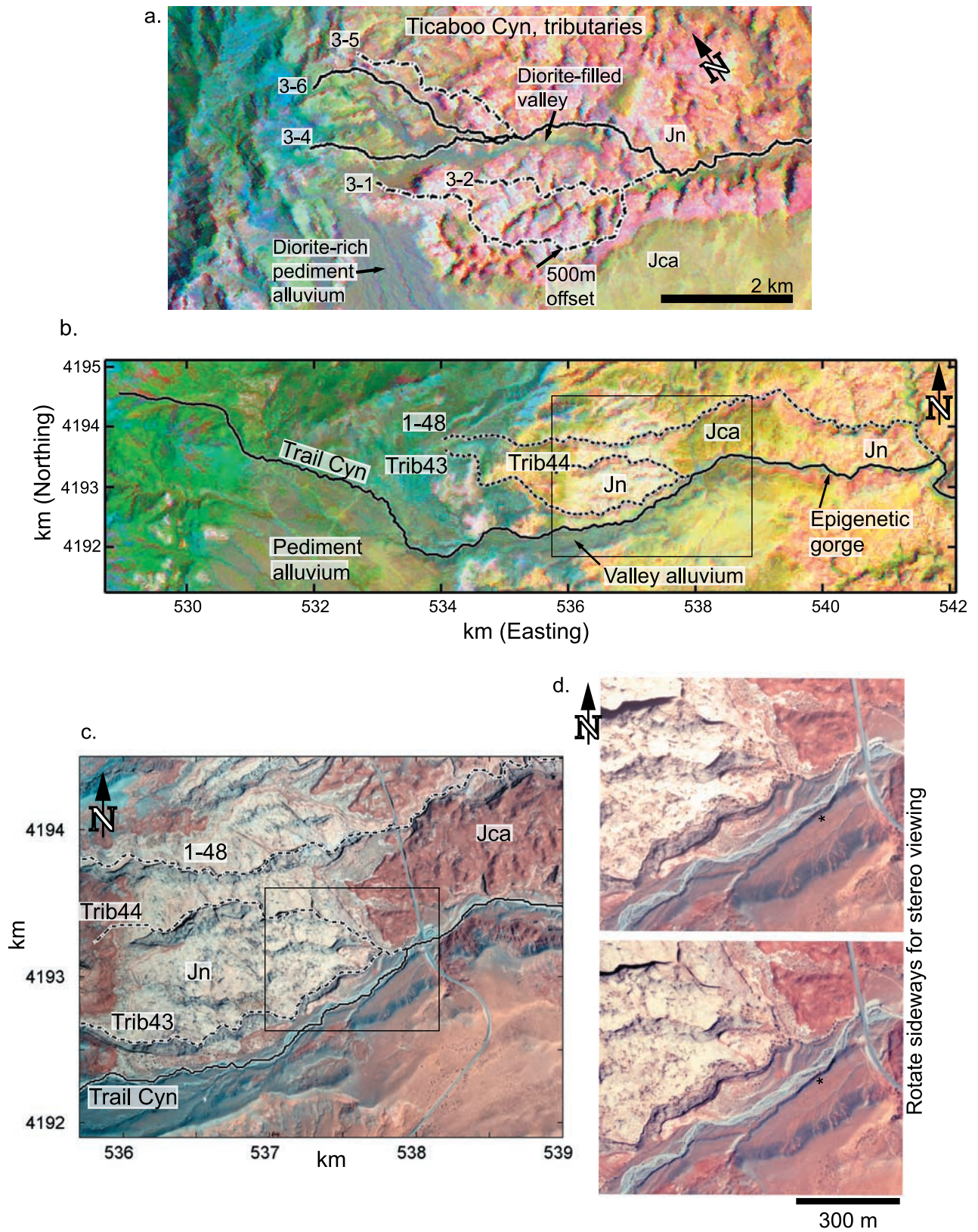
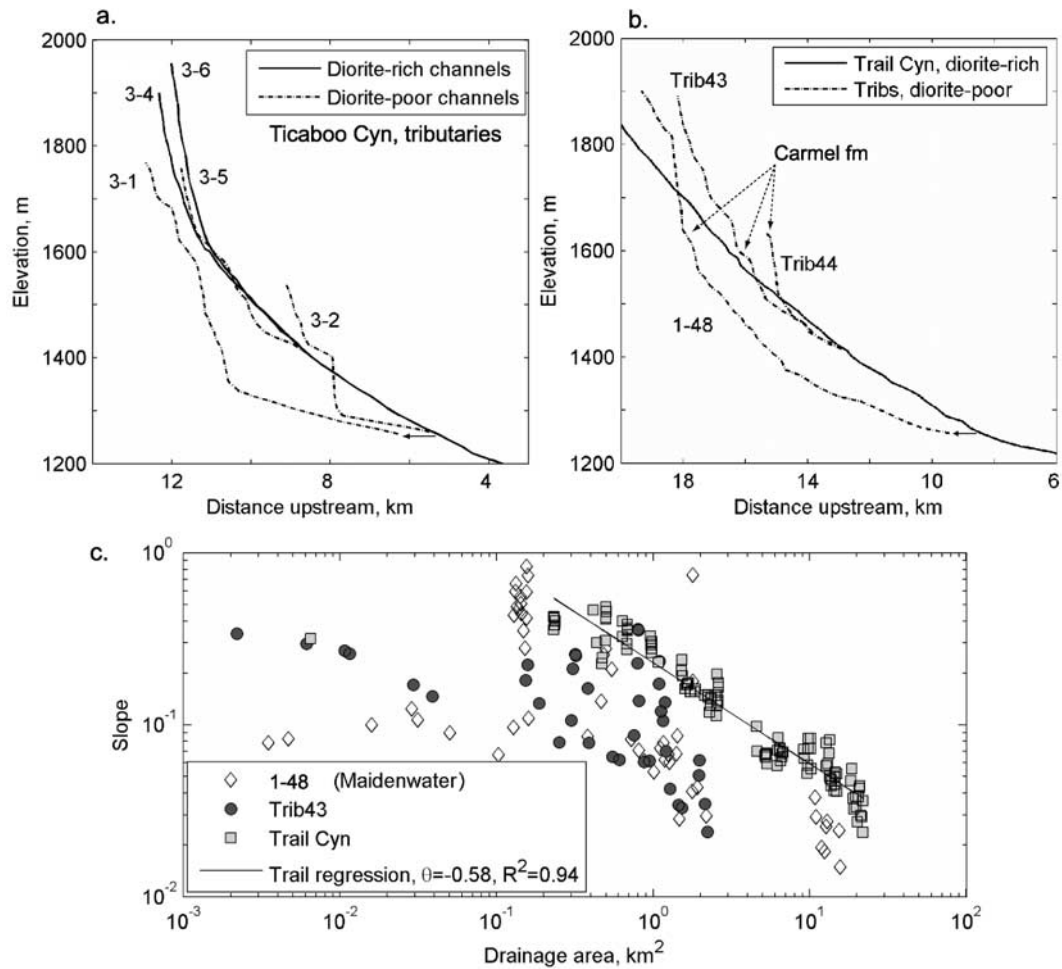


Figure 3



**Figure 4.** Channel profiles and slope area data. (a) Ticaboo Canyon profiles. Locations shown in Figure 3a. Channel 3–1 is offset by 1 km (x axis) for clarity. Near confluences, tributary slopes are lower than the main stem slope. (b) Trail Canyon, Trib43, Trib44, and 1–48 (Maidenwater); locations shown in Figure 3b. The tributary channels are incised more deeply to lower slopes than Trail Canyon in the vicinity of the confluences. Trail Canyon and 1–48 do not share a confluence directly but are both nearby tributaries of the larger Trachyte Creek. (c) DEM slope area data plotted for Trail Canyon, Trib43, and Maidenwater south. The diorite-poor channels have locally high slopes, but Trail Canyon has higher overall slopes at a given drainage area. Slopes were calculated over ~24.4 m of vertical elevation, which corresponded to two contour intervals in the original data (USGS 7.5' quadrangles; contour interval 40 feet). No other smoothing was done.

the basal part of the Navajo Sandstone as well as possible undermining due to other weathering and erosional processes such as groundwater seepage, as is sometimes observed near this stratigraphic contact [e.g., Howard and Kochel, 1988; Lamb et al., 2006]. Nonetheless, incision of the Ticaboo main stem has been inhibited by its abundant diorite gravel

bed load, preventing the river from exploiting a horizon of weak rock (Figure 4a). Bedrock exposed along the main stem channels of both Ticaboo Canyon and Trail Canyon indicates that the channels were not incised more deeply in the past.

**Figure 3.** Ticaboo Canyon and Trail Canyon. (a) Landsat image (bands 5, 4, 2, partially decorrelation stretched) of Ticaboo Canyon. Location shown in Figure 1. Channel traces are offset 500 m east to make the differences in alluvial fill between valleys more visible. Diorite pediments and valley fill appear gray, in contrast to the green (Jca, Carmel Formation) and pink (Jn, Navajo Sandstone) sedimentary bedrock units. (b) Landsat image showing Trail Canyon and diorite-poor tributaries. Location indicated in Figure 1. Photograph of epigenetic gorge in Figure 6c. (c) Aerial photograph showing Trail and Maidenwater canyons. Note the difference between Jca (dark red), Jn (tan), and diorite-rich alluvium (gray) filling the Trail Canyon valley. Location shown in Figure 4b (rectangle). (d) Stereo air photographs showing the confluences of Trail Canyon, Trib43, and Trib44. Location indicated in Figure 3c. To view in stereo, rotate the page 90° clockwise, relax your eyes, focus on infinity, and let the images overlap. The asterisk is the ~13 m fill terrace similarly marked in Figure 6. Note that the Trib43 channel elevations are lower than the adjacent Trail Canyon.



[29] Because lithologic heterogeneities and groundwater seepage may have influenced incision of the Ticaboo Canyon tributaries, we focus our analysis on Trail Canyon and surrounding channels. Figure 4c shows that DEM-derived slope area data for Trail Canyon are well fit by a power law as has been widely observed for both alluvial and bedrock channels [e.g., *Flint, 1974; Howard and Kerby, 1983; Howard et al., 1994; Wobus et al., 2006*]. In log-log space the power law relation  $S \sim A^{-\theta}$  plots as a straight line with slope  $-\theta$ , which is defined as the channel concavity index [e.g., *Whipple and Tucker, 1999*]. A regression through the Trail Canyon data gives  $\theta = -0.58$  ( $R^2 = 0.94$ ), which is within the range of concavities common for fluvial channels ( $\theta \sim -0.3$  to  $-0.7$ ) [*Whipple, 2004*]. Over most of their length, including the steeper headwater reaches, the smaller tributaries have more variable but lower slopes than Trail Canyon at comparable drainage areas. This is true not only for Trib43 and Maidenwater, but also for the other diorite-poor channels shown in Figures 2 and 4.

[30] We have observed that Trail Canyon receives snowmelt flow in some years in addition to flash floods, consistent with flow monitoring in a nearby channel [*Johnson et al., 2005*]. Owing to their lower headwater elevations the tributaries only receive flash floods. Precipitation rate increases with elevation in this landscape [*Gilbert, 1877; Hunt, 1953*], and so Trail Canyon can be thought of as effectively having greater discharge, relative to the tributaries, than is reflected in the differences in drainage area (Figure 4c). However, the elevation ranges of the surveyed main stem and tributary reaches are similar and so the frequency and intensity of flash flood rainfall events should be equivalent between channels over this elevation range. In addition, we interpret less efficient incision on Trail Canyon relative to the tributaries, even though the increase in discharge due to snowmelt would be expected to increase efficiency. Drainage area is therefore a conservative discharge proxy for comparing these channels. We do not further exaggerate the differences between channels by attempting to correct for increased precipitation with elevation.

[31] Upstream of the surveyed reach, Trail Canyon is modestly incised into colluvium and pediment deposits surrounding Mt Hillers, giving it an abundant supply of diorite sediment in addition to that stored in its valley (Figures 1 and 3b). On the basis of aerial photographs and Landsat imagery,  $94 \pm 3\%$  of the Trail Canyon watershed area upstream of the Trib43 confluence has surface cover of diorite bedrock, colluvium, pediment and valley fill. In contrast, the Trib43 watershed has  $21 \pm 5\%$  of its area covered by diorite, all upstream in the less incised headwaters. Trib44 has no diorite sources evident in its watershed. The supply of coarse diorite sediment likely decreases from Trail Canyon to Trib43 to Trib44. To summarize, the availability of diorite sediment supply correlates with differences in longitudinal profile smoothness and slopes. Slopes are steeper in the channels rich in coarse diorite sediment, especially when accounting for drainage area differences (Figure 4).

## 5.2. Field Surveys

[32] On the basis of the regional analysis, detailed field surveys were conducted along 7.3 km of Trail Canyon, 2.6 km of Trib43, 0.45 km of Trib44 and 2.0 km of the

south fork of Maidenwater Canyon (Figure 5a). Surveyed reaches correspond to DEM-derived drainage areas of 13.6 to 21.8 km<sup>2</sup> along Trail Canyon, 1.2 to 3.3 km<sup>2</sup> along Trib43, 0.7 to 1 km<sup>2</sup> along Trib44 and 1.8 to 12 km<sup>2</sup> along Maidenwater. The bedrock exposed in the surveyed reaches of the tributaries (43, 44) and Maidenwater is Navajo Sandstone. Downstream of the Trib43 confluence all of the bedrock exposed in Trail Canyon is Navajo Sandstone, whereas upstream of the trib43 confluence the active Trail Canyon channel is close to the contact between Navajo Sandstone and Carmel Formation, with Navajo Sandstone and rarely Carmel Formation exposed in the bed.

### 5.2.1. Channel Profiles

[33] Like the coarser-resolution DEM profiles, Figure 5b shows that (1) Trib43 and Trib44 have lower slopes than the main stem Trail Canyon and (2) Trail Canyon has less slope variability. Standard deviations ( $1\sigma$ ) of surveyed reach gradients (weighted for reach length) are 0.02, 0.05, 0.05 and 0.08 for Trail, Trib43, Trib44 and Maidenwater respectively, giving coefficients of variation (standard deviation divided by mean) of 0.4, 1.1, 2.9 and 2.0 respectively. These also serve as crude measurements of differences in bed roughness between the channels, and indicate that Trail Canyon is less rough at the reach scale than the others. Individual reaches were surveyed to capture changes in local slope, and the smoother profile of Trail Canyon is not an artifact of differences in reach lengths. Trib43, Trib44 and Maidenwater have impassable reaches with narrow slots, bedrock steps and boulder jams that restricted the total lengths of our surveys (Figure 5a). Trib44 has high slope variability due in part to a series of channel-spanning bedrock potholes. In contrast, as its name implies Trail Canyon provides the easiest access to the perennially flowing Trachyte Creek.

### 5.2.2. Channel Morphology

[34] Differences in channel morphology and bed cover are apparent at tributary junctions. Although both Trib43 and Trail Canyon have exposed Navajo Sandstone bedrock, the gray diorite sediment in Trail Canyon contrasts sharply with the bare bedrock in Trib43 (Figure 6a). Trib44 has essentially no coarse sediment on its bed, only sand, and has incised to a lower reach slope than boulder-laden Trib43 despite its smaller drainage area (Figure 6b).

[35] Trail Canyon tends to have a consistently flat bottom and rectangular cross section (Figure 7). Large boulders are occasionally present in the valley fill, and imbrication suggests that small boulders and cobbles are actively transported in the channel (Figure 7a). However, coarse sediment jams are almost never observed along Trail Canyon. Although we do not have independent quantitative measurements of bed roughness apart from standard deviations of surveyed reach gradients (section 5.2.1), field observations suggest that grain size is a large component of Trail Canyon bed roughness. Exposed bedrock tends to grade smoothly with surrounding alluvial cover rather than forming steps (Figures 6a and 7b). In contrast, Trib43 has bedrock steps and channel-spanning boulder jams (Figures 5, 6, and 7c). Sediment is sorted longitudinally, with sand and fine gravels just downstream of steps. Sediment coarsens downstream as the next bedrock step or boulder jam is approached. Maidenwater reach morphologies are similar to Trib43. Trib44 has very little coarse sediment and no boulder jams.

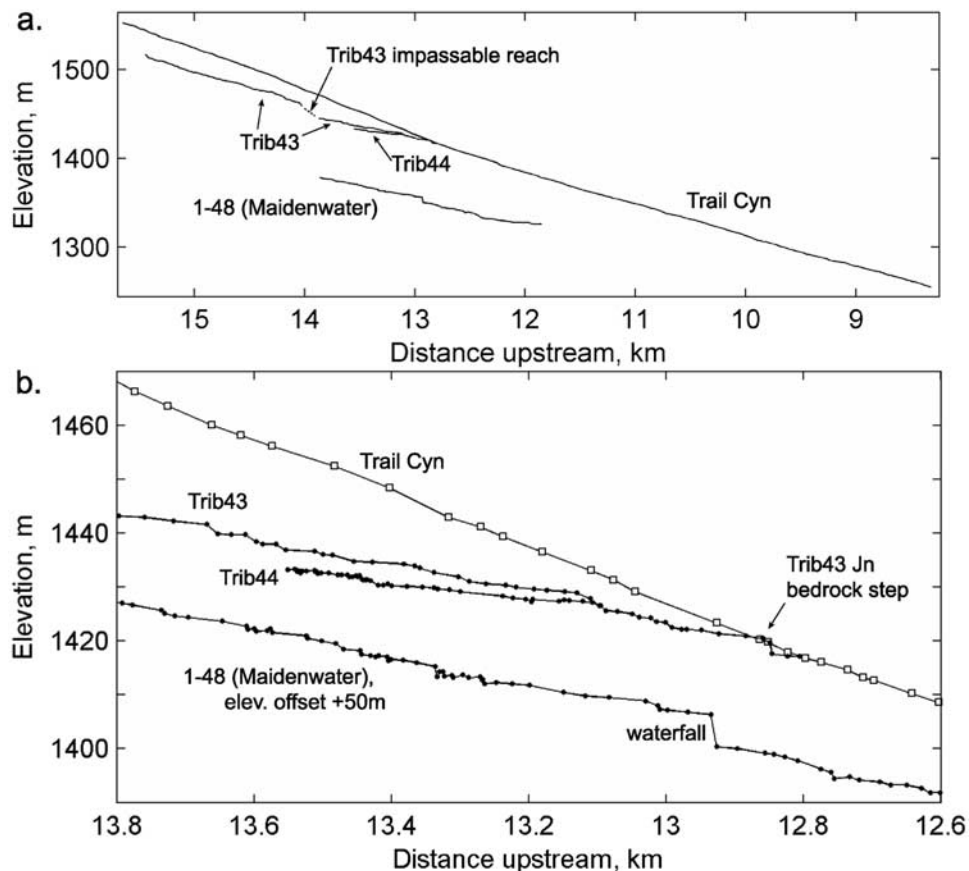


**Figure 5.** Field-surveyed channel profiles. (a) Complete distances surveyed along each channel. A steep impassable reach in Trib43 (dotted line,  $\sim 14$  km upstream, 150 m long) was not surveyed. (b) A close-up view of surveyed reaches, showing differences in slope and profile smoothness. Survey points were chosen to capture changes in local slope (described in section 4), and so the smoother profile of Trail Canyon is not an artifact of the wider sample spacing. The Trib43 bedrock step is shown in Figure 6a. Maidenwater Canyon has a 5 m waterfall where the channel crosses a small carbonate-rich bed within the Navajo Sandstone.

Bedrock in the Trib44 channel bottom appears fresh and is eroded into potholes and other sculpted forms, while bedrock above the active channel is more weathered (Figure 7d).

[36] Channel widths increase downstream but are highly variable and do not depend monotonically on drainage area (Figure 8). It is surprising that the mean widths of the different channels are similar since the Trail Canyon drainage area is five times larger than Trib43 and 30 times larger than Trib44. However, differences in channel morphology, sediment cover and bank material may influence the variability in widths. The Trail Canyon banks are mostly defined by coarse alluvium. The banks in Trib43 vary from sand to coarse diorite cobbles to bedrock, while in Trib44 the banks vary between sand and bedrock.

[37] Abundant bed cover was observed along all of the channels (Figure 8). Averaged over the surveyed distances, Trail, Trib43 and Trib44 have  $4\% \pm 2\%$ ,  $15\% \pm 5\%$  and  $35\% \pm 10\%$  bedrock exposed in the channel bed respectively. Uncertainties are 2 standard error ( $2S_e$ ); each distribution has a sufficient number of points so that  $2S_e$  approximately gives 95% confidence intervals on the mean amount of bedrock exposed in each channel. Bedrock

exposure in the channel banks is higher, with  $14 \pm 3\%$ ,  $52 \pm 6\%$  and  $64 \pm 10\%$  ( $2S_e$ ) exposed in the banks of Trail, Trib43 and Trib44, respectively (data not shown). Bedrock exposure in the bed decreases with increasing channel gradient ( $R^2 = 0.8$ ) (Figure 9).

### 5.2.3. Fill Terraces and Floodplains

[38] A terrace level about 13 m above the active channel is well preserved along Trail Canyon (Figures 3 and 6). Terraces of similar height are found along many sediment-rich channels including Ticaboo Canyon and Trachyte Creek. The fill terrace records the Trail Canyon valley slope during past aggradation, and is consistent with the present-day valley slope. In section 6, we interpret that the current channel slope is adjusted to transport its coarse sediment load, as would be the case during aggradation. Correlatable terrace remnants are not present in Trib43 or Trib44, perhaps owing to a lack of coarse sediment availability or a lack of subsequent preservation in the narrower tributary valleys.

[39] Figure 6c shows a location along Trail Canyon in which the terrace is preserved to the right of a bedrock knob, and the active channel now flows through the



**Figure 6.** Photographs comparing tributaries. (a) The view looking upstream at the confluence of Trail Canyon (left) and Trib43 (right) shows differences in coarse sediment bed cover between the channels. The lithologically controlled step in Trib43 is apparent in the field-surveyed profile (Figure 5). Stratigraphically, the step occurs close to the top of the Navajo Sandstone (Jn). Darker weathered beds of the Carmel Formation (Jca) form the hillslope above. The asterisk corresponds to a ~13 m fill terrace marked in Figure 3d. (b) Confluence of Trib43 and Trib44, showing more coarse sediment bed cover in Trib43. The 1.75 m laser pole is circled for scale. (c) Epigenetic gorge downstream in Trail Canyon, location shown in Figure 3b. Note field assistant for scale.

bedrock-walled slot to the left. The geometry indicates that, prior to terrace aggradation, the channel had cut down to approximately the same elevation as the present channel. When downcutting later occurred the channel reincised not

only through valley fill but although through bedrock that previously defined the valley margin, leaving a bedrock knob. This kind of feature has been termed an epigenetic gorge [Hewitt, 1998]. Several epigenetic gorges occur along



**Figure 7.** Field photographs showing channel morphology. (a) View upstream of the Trail Canyon channel. Note the imbricated cobbles in the foreground, the flat bed and rectangular channel cross section, and the active floodplain level with a higher fill terrace behind. The section of surveying rod visible is  $\sim 70$  cm. (b) Bedrock exposed in the Trail Canyon bed and bank, looking upstream, 1.75 m surveying rod. (c) Trib43, looking upstream. In the background, just upstream of where Jn bedrock narrows, is a steep boulder jam of diorite and sandstone boulders and cobbles. The foreground sediment is sand, illustrating longitudinal sorting. (d) Trib44, looking upstream, showing potholes and fluvial sculpting at the start of a narrow slot. All of the visible sediment is sand.

Trail Canyon [Ouimet *et al.*, 2008]. The more recent bedrock incision indicated by these features apparently has not influenced local channel slope, width or depth.

[40] Field observations suggest that bankfull flows in Trail Canyon occur on a regular basis, although we have no direct measurements of flood magnitudes or recurrence intervals. Trail Canyon has an active floodplain, particularly upstream where the valley is wide. Secondary channels with mud deposition and bent and twisted vegetation on the alluvial floodplain surface indicates recent flow above bankfull.

#### 5.2.4. Sediment Size Distribution

[41] Cumulative distributions of clasts  $\geq 3$  mm from Trail Canyon, Trib43 and Trib44 are statistically significantly different (Figure 10a). Alluvium ranging in size from sand to boulders can be found in both Trail Canyon and Trib43, but Trib43 has a broader distribution (less well sorted). We can reject the null hypothesis that the measured diameters

come from the same total distribution with  $>99\%$  confidence (two-sample Kolmogorov-Smirnov test) [Hayter, 1996]. However, the mean and median values of the distributions for Trail Canyon and Trib43 are not significantly different (T test with unequal variances [Wohl *et al.*, 1996]; Wilcoxon rank sum test). Sediment sizes are presented in millimeters but statistical comparisons were calculated using log-transformed values. Particles  $< 3$  mm (mostly sand) were omitted from the size distributions assuming that during relevant flows the fine sediment will be suspended and contribute little to bed load flux. Trail Canyon and Trib43 had similar total fractions of sand covering the bed (30% and 27% respectively). In contrast, we estimated in the field that the surface sediment in Trib44 was 98% sand. The Trail Canyon and Trib43 size distributions were measured by random walks, but the Trib44 distribution represents the coarse sediment trapped in two

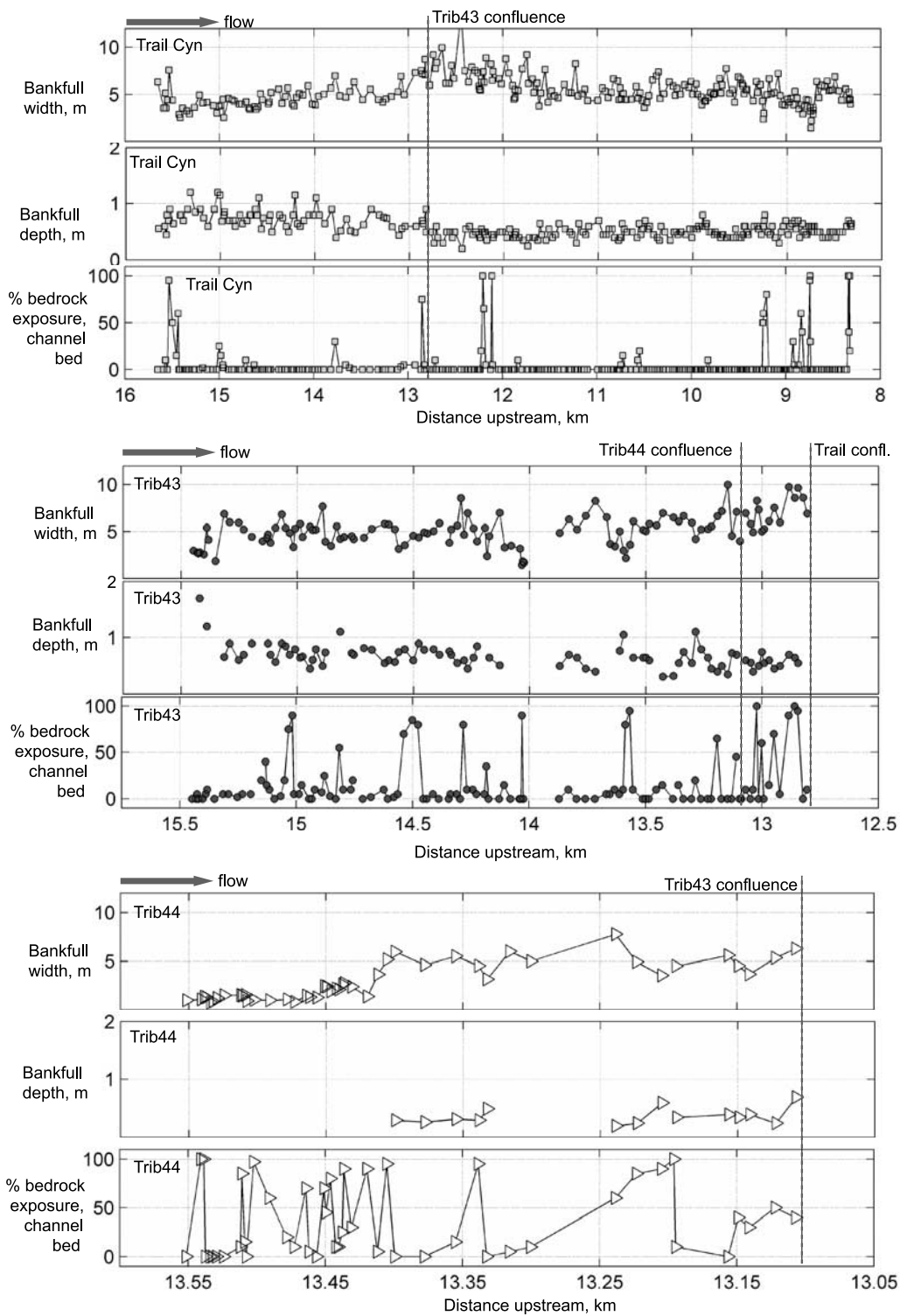


**Figure 8.** Surveyed bankfull width, depth, and percent bedrock exposure on the channel bed, covering the complete distances surveyed along each channel. Horizontal plot scales are different for each channel, but vertical scales are the same. Width decreases upstream of ~13.42 km along Trib44 because the channel enters the bedrock-walled slot shown in Figure 7d. Uncertainties are discussed in the text.

potholes as well as an isolated coarser patch measured by random walk in the channel.

[42] The Trail Canyon and Trib43 size distributions in Figure 10a represent amalgamations of pebble counts measured in separate channel reaches. In Trail Canyon, five

reaches of approximately 50 m each were spaced over 700 m of channel distance; the field survey demonstrated that channel longitudinal slope was constant over this distance. Approximately 100 clasts were measured in each reach (Figure 10b). An analysis of variance (ANOVA,  $\alpha = 0.05$ )

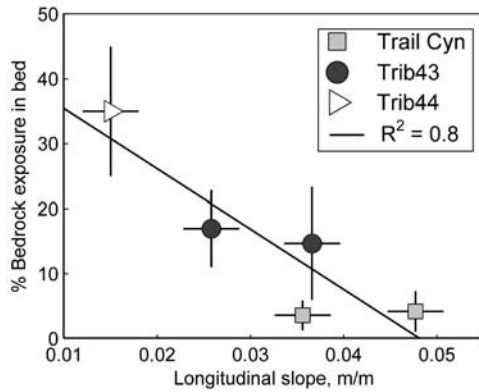


**Figure 9.** Reach-averaged slope plotted against percent bedrock exposure in the bed for Trib44 (distance upstream from Lake Powell 13.11 to 13.55 km), two reaches of Trib43 (12.81–13.87 km and 14.02–15.45 km upstream), and two reaches of Trail Canyon (upstream and downstream of the Trib43 confluence; 8.32–12.79 km and 12.82–15.65 km upstream). Together these reaches represent all of the surveyed distance along these channels (Figures 5 and 8).

demonstrates that the five distributions are statistically indistinguishable from one another, indicating negligible reach-scale longitudinal sorting along Trail Canyon.

[43] In contrast, sediment size distributions vary greatly between Trib43 reaches (Figure 10b). Point counts were conducted in 10 reaches along 256 m of the channel with no distance between adjacent reaches. Reach boundaries were chosen to capture local slope changes. Only ~50 clast diameters were measured in each reach. An analysis of variance ( $\alpha = 0.05$ ) allows us to reject the null hypothesis that the Trib43 reach size distributions are indistinguishable from one another, in contrast to the Trail Canyon reaches. Reach slope and  $D_{50}$  are correlated in Trib43, with slope explaining nearly 2/3 of the variation in  $D_{50}$  ( $R^2 = 0.63$ ) (Figure 10c). Longitudinal sediment sorting has formed boulder jams, bedrock steps and lower gradient reaches in Trib43.

[44] To constrain how diorite clasts contribute to the total coarse sediment load, clast lithologies were categorized as either diorite or sandstone (small numbers of resistant carbonate and chert clasts have been included in the sandstone distributions). In Trail Canyon, 79% of clasts  $\geq 3$  mm were diorite and 21% sandstone. In Trib43, diorite clasts comprise 52% of the coarse sediment, compared to 48% sandstone clasts. Surprisingly, diorite clasts in Trib43 are larger than in Trail Canyon (Trib43 diorite  $D_{50,dt} = 72$  mm,  $D_{90,dt} = 280$  mm, Trail Canyon diorite  $D_{50,dt} = 52$  mm,  $D_{90,dt} = 129$  mm), even though diorite clasts make up a smaller fraction of the Trib43 sediment load and less diorite is available in the Trib43 watershed. We cannot discount the possibility that Trib43 receives coarser diorite sediment, but it is unlikely considering that the progressive erosion of alluvium from pediment surfaces has been a key source of diorite clasts for both channels. We argue below that preferential transport of finer sediment from Trib43 has left a lag of coarse clasts.

### 5.3. Analysis of Trail Canyon: Critical Shear Stress, Sediment Flux, and Channel Gradient

[45] In this section, we calculate that thresholds for sediment motion are exceeded in Trail Canyon at flow depths well below bankfull, and we explore the degree to which Trail Canyon is graded to transport its sediment load. Boundary shear stress  $\tau_b$  is calculated assuming steady, uniform flow:

$$\tau_b = \rho_w g R S \quad (2)$$

where  $S$  is the downstreambed gradient (assumed equal to the water surface gradient),  $g$  is gravitational acceleration, and  $\rho_w$  is the density of water. The hydraulic radius  $R$  equals  $wd/(w + 2d)$  assuming a rectangular channel cross section. The Trail Canyon channel geometry is broadly consistent with the use of equation (2) because the channel has well-defined widths, rectangular cross sections, and little longitudinal or lateral sediment sorting (Figures 6, 7, and 10). Equivalent calculations are not presented for Trib43 because it has step-pools, highly variable slopes and strong longitudinal sediment sorting, all of which limit the application of these simple calculations [e.g., Zimmermann and Church, 2001; Yager et al., 2007].

[46] The shields stress  $\tau_b^*$  is a nondimensionalization of  $\tau_b$ :

$$\tau_b^* = \frac{\tau_b}{(\rho_s - \rho_w)gD} \quad (3)$$

where  $\rho_s$  is sediment density and  $D$  is a representative grain size, typically  $D_{50}$ . For Trail Canyon,  $D_{50} = 46$  mm and  $D_{90} = 120$  mm (Figure 10). For hydraulically rough flow, estimates of the critical shields stress ( $\tau_{cr}^*$ ) to initiate motion range from ~0.03 to 0.06 or higher for organized, armored beds [Zimmermann and Church, 2001]. The lack of bed armoring suggests a low value of  $\tau_{cr}^*$  [Reid et al., 1998] while the high channel slope suggests a high value [Lamb et al., 2008], so an average value of  $\tau_{cr}^* = 0.045$  is assumed.

[47] Volumetric bed load transport rate is calculated using the Fernandez Luque and van Beek [1976] bed load relation:

$$q_t = 5.7(r_b g D^3)^{0.5} (\tau_b^* - \tau_{cr}^*)^{1.5} \quad (4)$$

where  $q_t$  is sediment transport capacity per unit width ( $Q_t/w$ ) and  $r_b$  is the nondimensional buoyant density,  $(\rho_s/\rho) - 1$ . If bed load sediment is not supply limited then sediment flux per unit width  $q_s$  equals  $q_t$ . The limited work on sediment transport in flash flood-dominated systems suggests that sediment transport relations developed in other environments may be generally applicable. For a flash flood channel in Israel, Reid et al. [1998] found a best fit bed load relation that only varies from equation (4) a small amount in the prefactor (4.21 instead of 5.7), exponent (1.37 instead of 1.5) and  $\tau_{cr}^*$  (0.03).

[48] Field observations indicate that bankfull flow is common in Trail Canyon, and so we calculated shear stresses using surveyed values for local reach bankfull width, depth and slope. Figure 11a shows a histogram of excess Shields stress ( $\tau_b^*/\tau_{cr}^* - 1$ ) for  $D_{50}$  and  $D_{90}$  calculated

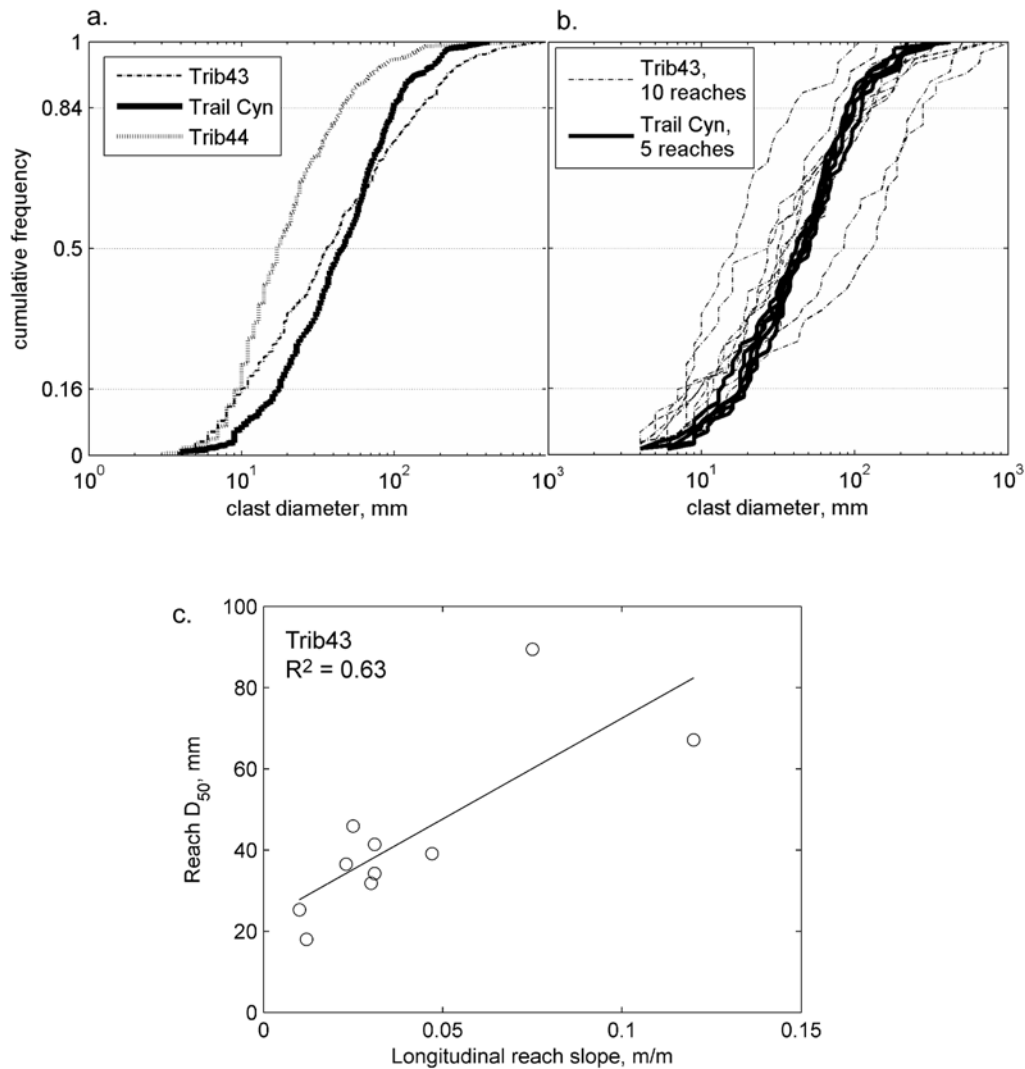


**Figure 10.** Pebble count sediment size distributions. (a) Total distributions (excluding sand) for each channel. Trail Canyon is better sorted than Trib43; both have larger coarse sediment (and much more of it) than Trib44. (b) Approximately 100 clast diameters were measured in each of 5 reaches of Trail Canyon, compared to  $\sim 50$  clasts measured in each of 10 reaches of Trib43. Slope-dependent longitudinal sorting is strong in Trib43 and negligible in Trail Canyon. (c) Longitudinal slope plotted against  $D_{50}$  for the 10 Trib43 reaches with separate pebble counts.

for bankfull flow in Trail Canyon. Because even  $D_{90}$  Shields stresses are higher than thresholds of motion ( $\tau_b^*/\tau_{cr}^* - 1 > 0$ ), essentially all sediment sizes exposed on the bed are calculated to move during bankfull flow in Trail Canyon. We note that the  $D_{90}$  Shields stress analysis gives a conservative upper bound on the initiation of  $D_{90}$  sediment transport: the combined effects of hiding and protrusion in grain mixtures would likely mean that the coarser bed sediment sizes would be transportable at lower stresses than predicted by this simple analysis [e.g., *Parker and Toro-Escobar*, 2002; *Wilcock and Crowe*, 2003].

[49] In addition to assuming bankfull flow conditions (Figure 11a), we also calculated the flow depth in each reach needed to reach the  $D_{50}$  threshold of motion along the channel on the basis of surveyed reach slope and width (Figure 11b). For 50% of the channel length, a flow depth of

just 8 cm or 11% of mean bankfull should overcome the  $D_{50}$  threshold of motion. Even when thresholds of motion are exceeded, all of the sediment on the bed would not necessarily be in motion, nor would more bedrock necessarily be exposed: in any given reach, the amount of sediment transported in from upstream in addition to sediment on the local bed and banks could exceed the local transport capacity. In addition to mobile bed load, static alluvium may be common along channel beds during floods even when thresholds of motion are greatly exceeded.

[50] Finally, we consider the relative importance of thresholds of motion and sediment flux in setting the slope of Trail Canyon. *Sklar and Dietrich* [2006] presented the following relations for the channel gradient necessary to overcome the threshold of motion ( $S_{cr}$ ) and the additional

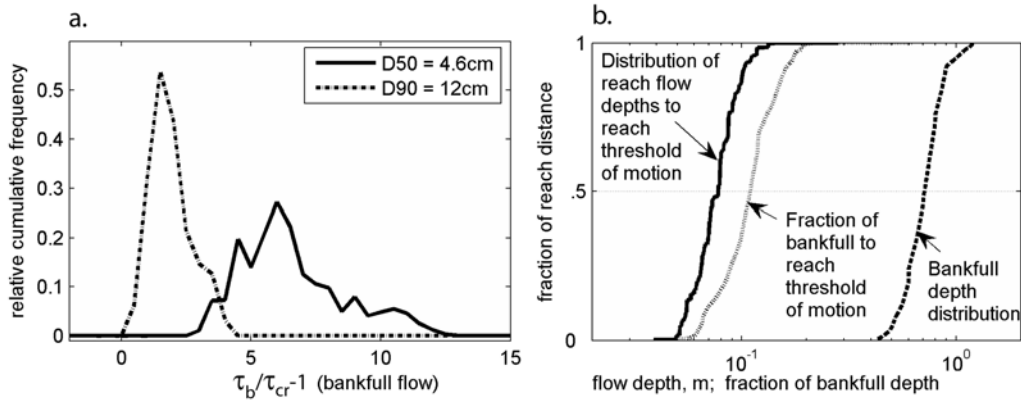


**Figure 11.** (a) Histograms represent the frequency of occurrence of excess Shield's stress ( $\tau_b^*/\tau_{cr}^* - 1$ ) per unit distance downstream (i.e., accounting for differences in surveyed reach lengths) calculated for bankfull flow in Trail Canyon. Zero corresponds to the threshold of motion. (b) Cumulative distribution of flow depth in each reach necessary to reach the threshold of motion. Also plotted are the distribution of measured bankfull depths and the ratio of these two; that is, the fraction of bankfull flow depth necessary to reach the threshold of motion. The flow depths necessary to initiate sediment motion are nearly an order of magnitude smaller than bankfull flow.

gradient component needed to transport the bed load flux supplied from upstream ( $\Delta S_{qs}$ ):

$$S_{cr} = \frac{\tau_{cr}^* r_b D}{R} \quad (5)$$

$$\Delta S_{qs} = \frac{r_b D}{R} \left( \frac{q_s}{5.7 \rho_s (r_b g D^3)^{0.5}} \right)^{2/3} \quad (6)$$

[51] Equation (5) is derived from (2) and (3), and (6) is a rearrangement of (4). In the saltation abrasion model, channel slope in excess of  $S_{cr} + \Delta S_{qs}$  contributes to bedrock erosion, and the gradient needed to erode bedrock at the steady state base level lowering rate can be calculated from the other components of equation (1):  $\Delta S_e = S - S_{cr} - \Delta S_{qs}$ . However, we limit our slope analysis to the relative importance of thresholds of motion versus sediment flux. Our field data do not provide sufficient constraints (e.g., intermittency of flow) to fully predict incision rates using the saltation-abrasion model.

[52] We have no field constraints on  $Q_s$  and so (6) is calculated assuming  $Q_s$  is 100%, 96% and 80% of transport capacity  $Q_t$ . The abundance of coarse, transportable sediment in the Trail Canyon channel and valley suggests that sediment supply is not limited and that  $Q_s$  is  $\sim 100\%$  of  $Q_t$  (see section 6). The 80% value is used as a conservative lower bound. The value of 96% is based on the linear cover term in the saltation-abrasion model:

$$Fe = 1 - \frac{Q_s}{Q_t} \quad (7)$$

where  $Fe$  is the fraction of bedrock exposed in the channel bed (1 - cover fraction). The use of equation (7) to calculate  $Q_s$  from  $Fe$  (surveyed at 4%) is internally consistent with the saltation-abrasion model [Sklar and Dietrich, 2004].

[53] Over the range of assumed  $Q_s$  values, we find that  $S_{cr}$  is less than half of the total channel slope for flow depths greater than  $\sim 20\text{--}25\%$  of bankfull, while  $\Delta S_{qs}$  is the

dominant contributor to total slope (Figure 12). Table 1 gives parameters used for these calculations. Note that when  $Q_s$  is 100% of  $Q_t$ ,  $S_{cr} + \Delta S_{qs} = S$  by definition. Nonetheless, the relative magnitudes of  $S_{cr}$  and  $\Delta S_{qs}$  suggest that over flow depths  $>25\%$  of bankfull depth, the fraction of slope that contributes to overcoming thresholds of motion is probably less than the fraction of slope that transports the sediment load supplied from upstream (Figure 12).

## 6. Discussion

[54] We draw four key findings from our field observations and sediment transport calculations:

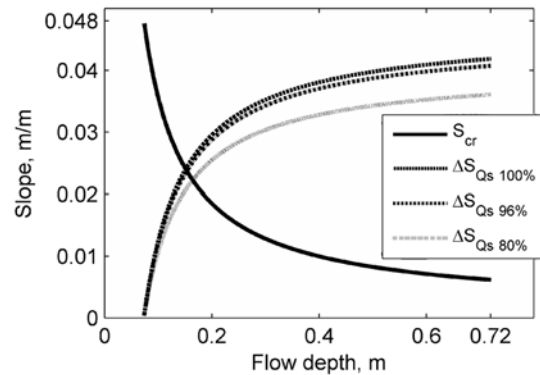


**Figure 12.** Components of total channel slope calculated using equations (5) and (6) as a function of flow depth based on reach-averaged Trail Canyon slope, width, and depth given in Table 1. At flow depths below  $\sim 0.08$  m the threshold of sediment motion (for  $D_{50} = 46$  mm) is not exceeded. At flow depths greater than  $\sim 0.18$  m, or  $\sim 25\%$  of bankfull flow, the fraction of slope transporting the sediment load ( $\Delta S_{qs}$ ) is larger than the fraction of slope that exceeds the threshold of sediment motion ( $S_{cr}$ ).



**Table 1.** Input Parameters and Values for Calculations in Figure 12<sup>a</sup>

Parameters for Trail Canyon Slope Component Calculations	Value	Input Parameter Source
Mean bankfull flow depth	0.72 m	field survey
Mean bankfull width	4.82 m	field survey
Mean slope ( $S$ )	0.048	field survey
$D_{50}$ (median grain size)	0.046 m	field survey
$\tau_{cr}$ (critical Shield's stress)	0.045	assumed
$\rho_s$ (sediment density)	2650 kg m <sup>-3</sup>	assumed
$\rho_w$ (water density)	1000 kg m <sup>-3</sup>	assumed
Calculated		
$q_t \times \rho_s$ at bankfull	101 kg s <sup>-1</sup> m <sup>-1</sup>	
$\tau_b$ at bankfull	261 Pa	
$\tau_b^*$ at bankfull	0.35	
$S_{cr}$ at bankfull	0.006	
Assuming $q_s/q_t = 1$		
$q_s \times \rho_s$ at bankfull	101 kg s <sup>-1</sup> m <sup>-1</sup>	
$\Delta S_{qs}$ at bankfull	0.042	
$\Delta S_e$ (i.e., $S - S_{cr} - \Delta S_{qs}$ )	0	
Assuming $q_s/q_t = 0.96$		
$q_s \times \rho_s$ at bankfull	97 kg s <sup>-1</sup> m <sup>-1</sup>	
$\Delta S_{qs}$ at bankfull	0.041	
$\Delta S_e$ (i.e., $S - S_{cr} - \Delta S_{qs}$ )	0.001	
Assuming $q_s/q_t = 0.8$		
$q_s \times \rho_s$ at bankfull	81 kg s <sup>-1</sup> m <sup>-1</sup>	
$\Delta S_{qs}$ at bankfull	0.036	
$\Delta S_e$ (i.e., $S - S_{cr} - \Delta S_{qs}$ )	0.006	

<sup>a</sup>Bankfull flow depth, width, slope, and sediment size are from field surveys of Trail Canyon, upstream of Trib43 confluence. Trail Canyon parameters upstream of confluence with Trib43 were used because this is where Trail Canyon point counts were measured.

[55] 1. Alluvial transport and deposition can greatly reduce the efficiency of river incision into bedrock, suggesting that river incision models should include cover effects.

[56] 2. Channel slope can be set mainly by the sediment load rather than bedrock properties, despite long-term incision into bedrock. The slope and morphology of sediment load-dominated channels adjust such that long-term transport capacity equals or barely exceeds long-term sediment flux.

[57] 3. High sediment transport rates can be more important than thresholds of coarse sediment motion for setting channel slope and inhibiting bedrock incision.

[58] 4. Alluvial cover inhibits incision not only when bed cover is complete, but also when moderate amounts of bedrock are exposed in channel beds.

[59] The key evidence that sediment cover can reduce the efficiency of incision (finding 1) is that sediment-starved tributaries have incised more deeply and to lower gradients than sediment-rich channels with larger drainage areas. This pattern of differential incision is consistent across the Henry Mountains landscape. *Hunt* [1953] recognized that Henry Mountains channels with abundant gravel maintained a steeper gradient than smaller tributaries with less coarse sediment: an observation that we rediscovered and exploit to validate cover effects in bedrock incision models. However, reduced erosional efficiency does not necessarily imply that cover-dominated incision is slow or that time scales of adjustment are long. In spite of abundant alluvium along Trail Canyon, bedrock is exposed in the channel bed and banks, the channel is largely contained in a bedrock canyon, and the smooth Trail Canyon channel profile

suggests that it has adjusted to the  $\sim 0.4$  mm a<sup>-1</sup> incision rate of Trachyte Creek, the sediment-rich channel that sets the base level of Trail Canyon (Figures 1 and 2) [*Cook et al.*, 2009]. Several unique factors of this field site enable our analysis. The coarse sediment load varies systematically and independently from bedrock lithology. We eliminate lithologic complexities by only comparing channel reaches that are incised into Navajo Sandstone. Because Trail Canyon, Trib43 and Trib44 share tributary junctions and meet at grade, the local rate of base-level fall for all three is essentially the same. Furthermore, plausible landscape disequilibrium dictates that the Trail Canyon incision rate must be less than or equal to that along the tributaries.

[60] In the remainder of section 6, we first argue that sediment in Trail Canyon is not supply limited and that terraces and the smooth channel profile are consistent with long-term  $Q_s \sim Q_t$ . Next, we qualitatively evaluate several proposed cover models on the basis of our field observations. We interpret how sediment supply to the tributaries may have changed over the time scales of differential incision between the compared channels. Finally we discuss possible mechanisms by which cover effects may occur, including temporal changes in cover, high mobile sediment fluxes, thresholds of motion, and increases in bed roughness and changes in channel morphology which reduce the transport capacities of flows.

## 6.1. Sediment Supply and the Gradient of Trail Canyon

[61] We interpret that the longitudinal slope of Trail Canyon is dominantly set by the coarse sediment it transports and that  $Q_s \sim Q_t$ , making it a sediment load-dominated bedrock channel as defined in section 2. Several lines of evidence suggest that the channel slope and morphology are primarily adjusted to transport the sediment load. First, sediment supply is not limited because ample coarse sediment is available for entrainment and transport from the channel bed, banks, floodplain and watershed (Figures 7 and 8).

[62] Second, the fill terrace  $\sim 13$  m above the active Trail Canyon channel (Figures 3 and 6) records that the valley slope during aggradation, when the channel would have been entirely alluvial and its slope adjusted to transport its sediment supply, is the same as the valley slope found today. Presumably some combination of forcing factors and channel response (discharge frequency/magnitude, sediment flux, slope, channel morphology and sinuosity) were different during aggradation, although  $\sim 13$  m of aggradation is modest. Nonetheless, similar valley slopes during aggradation suggest that the current channel slope and morphology are set primarily by the sediment load.

[63] Third, the smooth profile of Trail Canyon supports the interpretation that its gradient is adjusted to transport the sediment load. The longitudinal profiles of Trail Canyon and similar sediment-rich channels are smoother than sediment-poor tributaries (Figures 2, 4, and 5). Slope breaks do not occur at lithologic contacts. As discussed previously, models of sediment load-dominated channel incision predict that local incision will depend on the sediment supply from the entire upstream drainage area, rather than on local bedrock properties [*Whipple and Tucker*, 2002]. With only 4% bedrock exposed on the bed and 15% on the banks of

Trail Canyon, we cannot demonstrate that the bedrock surface underlying alluvium is necessarily as smooth as the current profile. However, where bedrock is exposed along Trail Canyon it tends to grade smoothly with the alluvial channel bed, in contrast to bedrock exposed in Trib43 and Trib44 (Figures 6 and 7). Epigenetic gorges similarly indicate that more recent bedrock incision does not perturb the local channel gradient (Figure 6c).

## 6.2. Model Evaluation

[64] Incision models that do not include cover effects, and cover models in which sediment only inhibits bedrock incision when  $Q_s \geq Q_t$ , are inconsistent with our data. As discussed, the comparison of Trail Canyon and Trib43 establishes that bedrock incision is strongly inhibited at high sediment load. The comparison of Trib43 and Trib44 suggests that the sediment load of channels can reduce the efficiency of bedrock incision even when moderate amounts of bedrock are exposed in channels.

[65] With limited quantitative constraints on key variables, our data are not sufficient to distinguish between cover models that reduce erosional efficiency for  $Q_s < Q_t$ , including models of *Beaumont et al.* [1992], *Sklar and Dietrich* [1998, 2004], and *Turowski et al.* [2007c]. All three models predict that channel gradient will increase with sediment flux, predict negative trends between the extent of cover and  $Q_s/Q_t$ , and predict an increase in equilibrium channel gradient with decreasing bedrock exposure. All of these predictions are qualitatively consistent with our data (Figure 9). Direct field evaluations of cover models that are different in detail but predict similar trends may require tight constraints on long-term  $Q_s$ ,  $Q_t$ , alluvial cover, erosion rate and the magnitude-frequency distribution of floods.

[66] Our comparison of channels validates the cover effect but neither supports nor contradicts the tools effect. The tools effect would only be supported by direct or indirect evidence that an increase in sediment flux increased erosional efficiency [*Sklar and Dietrich*, 2004, 2006]. The smooth profiles of Trail Canyon and other sediment load-dominated channels suggest that when patches of bedrock become exposed in the channel bed, local incision due to sediment impacts may be rapid and efficient. However, beyond being consistent with field observations that bed load abrasion by is the dominant erosion mechanism, the smooth profiles do not constrain the tools effect or its systematics. One reason that tools effects are not expressed may be that the slope of each channel is effectively adjusted to the local sediment supply (i.e., the cover effect is dominant). Channels which are locally sediment-starved and undergoing strongly transient incision may be most useful for evaluating tools effects [e.g., *Crosby et al.*, 2007; *Cowie et al.*, 2008].

## 6.3. Cover Effects: Temporal Controls

[67] Long-term landscape erosion has progressively removed pediments which previously covered the region more extensively [*Gilbert*, 1877; *Hunt*, 1953], transporting the surface veneer of diorite alluvium through the fluvial system. Over time scales of local pediment stripping (~100 ka) the coarse sediment supply to Trib43 and Trib44 must have decreased. While we do not know how strongly this timing coincides with differential bedrock incision

between these tributaries and Trail Canyon, we interpret that the differential incision reflects abundant coarse sediment supply in Trail Canyon, reduced supply to Trib43 and negligible supply to Trib44. If channel slope and morphology respond rapidly to small changes in sediment supply, then tributary slopes may have effectively remained adjusted to the decreasing sediment supply. If however the sediment supply was exhausted more rapidly than channel slope and morphology could adjust, then these tributaries may currently be incising somewhat more rapidly than the trunk stream of Trail Canyon. Unlike along Trail Canyon, diorite sediment supply and local channel incision are currently decoupled on the tributaries, and changes in tributary incision rates will minimally affect the supply rate of coarse diorite sediment. This decoupling allows sediment supply to vary among channels with the same base level control and leads to the differences in erosional efficiency that we interpret.

[68] Uncertainties remain in understanding how alluvial cover actually reduces the efficiency of incision. We have no direct constraint on the relative importance of temporal compared to spatial variations in cover. During fill terrace aggradation along Trail Canyon, bedrock would not have been exposed. Terraces are not currently found along Trib43 or Trib44, perhaps because insufficient sediment was available to enable aggradation. It is plausible that a reduction in time over which bedrock was exposed in Trail Canyon compared to the tributaries has been dominant in reducing long-term erosional efficiency. If incision occurs rapidly when bedrock is exposed, then channels may rapidly become sediment load dominated and periods of aggradation may not greatly affect river slope during periods of incision. These conditions would be favored by weak bedrock and abundant coarse sediment supply [*Sklar and Dietrich*, 2006], as are found along Trail Canyon. However, if bedrock is very strong or sediment supply is limited, then a channel may take longer to adjust to the condition where sediment load controls channel slope, and periods of aggradation may reduce the long-term incision rate (or be reflected in steeper channel slopes).

[69] At shorter time scales, variable discharge will lead to spatial and temporal variability in local sediment supply, transport capacity and bedrock exposure during individual floods. Our data only constrain spatial differences in cover between channels at a moment in time. Bed cover and other aspects of channel morphology fluctuate to an undetermined degree during and between floods, and over decadal to millennial time scales. We assume that this temporal variability is smaller than the differences in bed cover and sediment supply between Trail Canyon, Trib43 and Trib44.

[70] Channel morphology, long-term sediment flux and long-term incision rates reflect the combined influence of many flow events of different magnitudes [e.g., *Parker and Toro-Escobar*, 2002; *Snyder et al.*, 2003; *Hartshorn et al.*, 2002; *Lague et al.*, 2005; *Turowski et al.*, 2007a]. In the cover formulation of the saltation-abrasion model (equation (7)), bed cover is complete at  $Q_s = Q_t$  and no incision can occur. However, in natural channels the variations in flood magnitude and sediment flux will cause temporal and spatial variations in local  $Q_s$  and local  $Q_t$ , sometimes exposing bedrock and allowing local incision. Discharge and sediment flux variability provide a mecha-

nism by which a channel may remain at long-term  $Q_s/Q_t \sim 1$  and still incise.

#### 6.4. Cover Effects: Relationships Among Sediment Supply, Transport Capacity and Bed Roughness

[71] We hypothesize that the different morphologies of the channels we compare result from feedbacks between sediment supply and incision, influencing ways in which sediment actually reduces erosional efficiency. Along Trail Canyon, calculations indicate that thresholds of motion are exceeded over most flow depths, making this a “live bed” gravel channel in which bed load transport is common [Howard, 1998]. Therefore, alluvial cover and inhibition of incision can result from a high flux of bed load. Local deposition will occur if the local sediment volume per unit bed area exceeds the local transport capacity of the flow, even if thresholds of motion are greatly exceeded. Abrasion can be inhibited by “static” cover, i.e., stable alluvial deposition on the local channel bed. In addition, Turowski *et al.* [2007c] hypothesized that “dynamic” cover effects may reduce local incision when the concentration of bed load in active transport over bare bedrock is sufficiently high. Our data cannot distinguish between static or dynamic cover mechanisms for Trail Canyon.

[72] In contrast to Trail Canyon, the morphology of Trib43 suggests that cover effects in this channel occur owing to increasing bed roughness and thresholds of motion. The only direct constraint we have on bed roughness is the variability in surveyed reach slopes (section 5.2.1). Nonetheless, isolated large boulders (Figure 6b) and organized boulder jams (Figure 7c) suggest that rarely mobile lag deposits have developed and that thresholds of motion are important in Trib43. Diorite clasts in Trib43 are larger than in Trail Canyon, suggesting that smaller diorite clasts have been preferentially transported out of Trib43. As sediment supply is reduced, bed roughness may increase owing to the winnowing of smaller sediment, the coarsening of surface layers and the development of boulder jams, bedrock steps, and lower gradient reaches in between. An increase in bed roughness will increase form drag and decrease the transport capacity of the flow [e.g., Yager *et al.*, 2007]. The coarse tail of the Trib43 grain size distribution may be dominant in covering bedrock and reducing the efficiency of incision.

[73] The differences between Trail Canyon, Trib43 and Trib44 show how bed roughness, channel morphology and gradient adjust through feedbacks to differences in relative sediment supply. As coarse sediment supply decreases, we envision a transition from plane bed Trail Canyon to Trib43 as the bed becomes longitudinally sorted and organized into steep coarse reaches separated by lower slope reaches of finer sediment. Montgomery and Buffington [1997] developed a conceptual model for mountain channels in which reach morphology varies as a function of  $Q_s/Q_t$ . At  $Q_s/Q_t \sim 1$  they predict plane bed morphology, consistent with Trail Canyon. At lower  $Q_s/Q_t$ , step-pools are predicted to form as the bed material coarsens owing to selective transport and increases in roughness owing to bed sorting into steps, consistent with Trib43. In Trib44, bedrock steps and pot-holes contribute to bed roughness, but coarse sediment is not available to form boulder jams.

[74] Transport capacity may not be the best variable for parameterizing alluvial cover, because it depends not only on channel slope and discharge but also on width, roughness and sediment supply [e.g., Montgomery and Buffington, 1997; Chatanantavet and Parker, 2008]. Channel morphology can rapidly adjust, through feedbacks, to transport the coarse sediment load. In other words,  $Q_t$  may often be a function of  $Q_s$  rather than the other way around [Mackin, 1948]. Without including feedbacks between bed roughness, channel morphology and transport capacity, parameterizing bed cover as a function of  $Q_s/Q_t$  is incomplete. For example, Turowski *et al.* [2007c] argue that if  $Q_s$  is even slightly smaller than  $Q_t$ , the small amount of excess transport capacity will entrain additional sediment, increase the amount of bedrock exposed, reduce the amount of local sediment available for entrainment, and lead to full bedrock exposure with zero static alluvial cover. However, this argument assumes that transport capacity does not change substantially as sediment is entrained and bed morphology changes, and also that thresholds of motion are exceeded for the complete distribution of sediment sizes supplied to the channel. These conditions do not appear to be met along Trib43. Bed roughness changes are similarly not explicitly included in the cover term of the saltation-abrasion model (equation (7)) [Sklar and Dietrich, 2004].

[75] Recent flume experiments on bedrock incision illustrate how alluvial cover and transport capacity vary with evolving bed roughness. Chatanantavet and Parker [2008] explored feedbacks between roughness and alluviation when the dominant roughness element was deposited sediment rather than bedrock topography. By independently controlling sediment flux and water discharge, Johnson and Whipple [2007] set flume-averaged  $Q_t$  to be much greater than  $Q_s$ . However, bed roughness increased owing to localized incision while the topographically controlled width of active sediment transport decreased, resulting in locally decreased transport capacity and locally increased  $Q_s$ . Both Johnson and Whipple [2007] and Finnegan *et al.* [2007] found that bedrock bed morphologies reached a condition of  $Q_s \sim Q_t$  primarily owing to width and bed roughness adjustments, but also continued to incise. Changes in channel width and roughness occurred much faster than changes in slope, but gravity continued to preferentially focus erosion processes downward. In natural channels undergoing transient incision by abrasion, we envision a relatively rapid approach to sediment load-dominated conditions caused by changes in width and roughness, followed by a continued but slower adjustment of channel slope resulting from vertical incision at long-term  $Q_s \sim Q_t$ .

#### 6.5. Future Research Questions

[76] Many uncertainties remain in understanding not only how alluvial cover affects bedrock channel incision, but also how mountain rivers respond to hydrological and base level forcing:

[77] 1. What are the feedbacks between bed roughness, channel morphology, sediment supply, sediment transport, grain size distribution, and discharge? How should these interactions be modeled?

[78] 2. How does bed cover vary during flood events and with underlying bedrock topography? What is the relative

importance of spatial compared to temporal variations in cover, and of static (immobile) versus dynamic (mobile) cover effects [Turowski et al., 2007c]?

[79] 3. How should cover effects be modeled over a range of time scales? What field data are needed to further discriminate between proposed models?

[80] 4. Over what range of parameter space do tools effects dominate [e.g., Cowie et al., 2008]?

## 7. Conclusions

[81] Patterns of differential channel downcutting in the Henry Mountains, Utah, support the following key interpretations:

[82] 1. Alluvial transport and deposition can greatly reduce the efficiency of river incision into bedrock, validating hypothesized “cover effects” of the sediment load of channels. To recreate patterns of channel incision in this landscape, bedrock incision models would require a cover term.

[83] 2. Channel slope can be set mainly by sediment load rather than bedrock properties, despite long-term incision into bedrock. We propose the term “sediment load dominated” to describe bedrock channels in which slope and morphology have adjusted, through feedbacks, so that long-term transport capacity equals or barely exceeds long-term sediment flux. Sediment load–dominated channels can still incise bedrock, in part because of short-term variability in local  $Q_s/Q_t$ .

[84] 3. High sediment transport rates can be more important than thresholds of coarse sediment motion for setting channel slope and limiting bedrock incision. Calculations suggest that the slope of a particular sediment load–dominated bedrock channel (Trail Canyon) is probably set by sediment flux, because abundant sediment is available for transport and shear stress thresholds to initiate sediment motion are greatly exceeded at flow depths well below bankfull. Conversely, in a nearby channel with a reduced sediment supply (Trib43), we interpret that thresholds of motion, and reductions in transport capacity associated with increased reach-scale bed roughness, are probably the dominant cover effects.

[85] 4. Alluvial cover inhibits incision not only when bed cover is complete, but also when moderate amounts of bedrock are exposed in channel beds. We can reject simple models in which cover only prevents incision when the bed is completely covered, but our data are not sufficient to quantitatively differentiate between proposed equations for cover effects with partial bed cover.

[86] **Acknowledgments.** We thank many people for assistance collecting field data, including Wayne Baumgartner, Jessica Black, Mariela Perignon, and Kyle Straub. Nathan Niemi and Benjamin Crosby developed Arcpad scripts used for data collection. Joe Farrow measured rock strengths and erodibilities. Detailed reviews by Jens Turowski, Dimitri Lague, Paul Bishop, and Associate Editor Brian McArdell improved the manuscript significantly. This work was supported by NSF Geomorphology and Land Use Dynamics grants EAR-0345622 and EAR-0345344.

## References

Beaumont, C., P. Fullsack, and J. Hamilton (1992), Erosional control of active compressional orogens, in *Thrust Tectonics*, edited by K. R. McClay, pp. 1–18, Chapman and Hall, New York.

Brocard, G. Y., and P. A. van der Beek (2006), Influence of incision rate, rock strength, and bedload supply on bedrock river gradients and valley-

flat widths: Field-based evidence and calibrations from western Alpine rivers (southeast France), in *Tectonics, Climate, and Landscape Evolution*, edited by S. D. Willett et al., *Spec. Pap. Geol. Soc. Am.*, 398, 101–126, doi:10.1130/2006.2398(07).

Chatanantavet, P., and G. Parker (2008), Experimental study of bedrock channel alleviation under varied sediment supply and hydraulic conditions, *Water Resour. Res.*, 44, W12446, doi:10.1029/2007WR006581.

Cook, K. L., K. X. Whipple, A. M. Heimsath, and T. C. Hanks (2009), Rapid incision of the Colorado River in Glen Canyon: Insights from channel profiles, local incision rates, and modeling of lithologic controls, *Earth Surf. Processes Landforms*, doi:10.1002/esp.1790, in press.

Cowie, P. A., A. C. Whittaker, M. Attal, G. Roberts, G. E. Tucker, and A. Ganas (2008), New constraints on sediment-flux-dependent river incision: Implications for extracting tectonic signals from river profiles, *Geology*, 36(7), 535–538, doi:10.1130/G24681A.1.

Crosby, B. T., K. X. Whipple, N. M. Gasparini, and C. W. Wobus (2007), Formation of fluvial hanging valleys: Theory and simulation, *J. Geophys. Res.*, 112, F03S10, doi:10.1029/2006JF000566.

Davis, W. M. (1889), Rivers and valleys of Pennsylvania, *Natl. Geogr. Mag.*, 1, 183–253.

Davy, P., and A. Crave (2000), Upscaling local-scale transport processes in large-scale relief dynamics, *Phys. Chem. Earth*, 25(6–7), 533–541, doi:10.1016/S1464-1895(00)00082-X.

Fernandez Luque, R., and R. van Beek (1976), Erosion and transport of bed-load sediment, *J. Hydraul. Res.*, 14, 127–144.

Finnegan, N. J., L. S. Sklar, and T. K. Fuller (2007), Interplay of sediment supply, river incision, and channel morphology revealed by the transient evolution of an experimental bedrock channel, *J. Geophys. Res.*, 112, F03S11, doi:10.1029/2006JF000569.

Flint, J. J. (1974), Stream gradient as a function of order, magnitude, and discharge, *Water Resour. Res.*, 10, 969–973, doi:10.1029/WR010i005p00969.

Garvin, D. C., T. C. Hanks, R. C. Finkel, and A. M. Heimsath (2005), Episodic incision of the Colorado River in Glen Canyon, Utah, *Earth Surf. Processes Landforms*, 30, 973–984, doi:10.1002/esp.1257.

Gilbert, G. K. (1877), *Report on the Geology of the Henry Mountains*, 106 pp., Gov. Print. Off., Washington, D. C.

Hancock, G. S., and R. S. Anderson (2002), Numerical modeling of fluvial strath-terrace formation in response to oscillating climate, *Geol. Soc. Am. Bull.*, 114, 1131–1142.

Hanks, T. C., I. Lucchitta, S. W. Davis, M. E. Davis, R. C. Finkel, S. A. Lefton, and C. D. Garvin (2001), The Colorado River and the age of Glen Canyon, in *Colorado River Origin and Evolution: Proceedings of a Symposium Held at Grand Canyon National Park in June, 2000*, *Grand Canyon Assoc. Monogr.*, vol. 12, edited by R. A. Young and E. E. Spammer, pp. 129–134, Grand Canyon Assoc., Grand Canyon, Ariz.

Hartshorn, K., N. Hovius, W. B. Dade, and R. L. Slingerland (2002), Climate-driven bedrock incision in an active mountain belt, *Science*, 297, 2036, doi:10.1126/science.1075078.

Hayter, A. J. (1996), *Probability and Statistics for Engineers and Scientists*, PWS, Boston, Mass.

Hewitt, K. (1998), Catastrophic landslides and their effects on the upper Indus streams, Karakorum Himalaya, northern Pakistan, *Geomorphology*, 26, 47–80, doi:10.1016/S0169-555X(98)00051-8.

Hintze, L. F., and W. L. Stokes (1963), Geologic map of Utah southeast quarter, scale 1:250000, Utah State Land Board, Salt Lake City.

Hintze, L. F., G. C. Willis, D. Y. M. Laes, D. A. Sprinkel, and K. D. Brown (2000), *Digital Geologic Map of Utah*, Utah Geol. Surv., Salt Lake City.

Howard, A. D. (1998), Long profile development of bedrock channels: Interaction of weathering, mass wasting, bed erosion, and sediment transport, in *Rivers Over Rock: Fluvial Processes in Bedrock Channels*, *Geophys. Monogr. Ser.*, vol. 107, edited by K. J. Tinkler and E. E. Wohl, pp. 297–319, AGU, Washington, D. C.

Howard, A. D., and G. Kerby (1983), Channel changes in Badlands, *Geol. Soc. Am. Bull.*, 94, 739–752, doi:10.1130/0016-7606(1983)94<739:CCIB>2.0.CO;2.

Howard, A. D., and R. C. Kochel (1988), Introduction to cuesta landforms and sapping processes on the Colorado Plateau, in *Sapping Features of the Colorado Plateau: A Comparative Planetary Geology Field Guide*, edited by A. D. Howard et al., *NASA Spec. Publ.*, SP-491, 6–56.

Howard, A. D., M. A. Seidl, and W. E. Dietrich (1994), Modeling fluvial erosion on regional to continental scales, *J. Geophys. Res.*, 99, 13,971–13,986, doi:10.1029/94JB00744.

Hunt, C. B. (1953), Geology and geography of the Henry Mountains region, Utah, *U.S. Geol. Surv. Prof. Pap.*, 228, 234 pp.

Jackson, M. D., and D. D. Pollard (1990), Flexure and faulting of sedimentary host rocks during growth of igneous domes, Henry Mountains, Utah, *J. Struct. Geol.*, 12, 185–206, doi:10.1016/0191-8141(90)90004-I.

Jansen, J. D. (2006), Flood magnitude-frequency and lithologic control on bedrock river incision in post-orogenic terrain, *Geomorphology*, 82, 39–57, doi:10.1016/j.geomorph.2005.08.018.

- Johnson, J. P. (2007), Feedbacks between erosional morphology, sediment transport and abrasion in the transient adjustment of fluvial bedrock channels, Ph.D. dissertation, Mass. Inst. Technol., Cambridge.
- Johnson, J. P., and K. X. Whipple (2007), Feedbacks between erosion and sediment transport in experimental bedrock channels, *Earth Surf. Processes Landforms*, *32*, 1048–1062, doi:10.1002/esp.1471.
- Johnson, J. P., K. X. Whipple, and L. S. Sklar (2005), Field monitoring of bedrock channel erosion and morphology, *Eos Trans. AGU*, *86*(52), Fall Meet. Suppl., Abstract H52A–01.
- Kelsey, M. R. (1990), *Hiking and Exploring Utah's Henry Mountains and Robbers Roost*, 224 pp., Kelsey, Provo, Utah.
- Lague, D., A. Crave, and P. Davy (2003), Laboratory experiments simulating the geomorphic response to tectonic uplift, *J. Geophys. Res.*, *108*(B1), 2008, doi:10.1029/2002JB001785.
- Lague, D., N. Hovius, and P. Davy (2005), Discharge, discharge variability, and the bedrock channel profile, *J. Geophys. Res.*, *110*, F04006, doi:10.1029/2004JF000259.
- Lamb, M. P., A. D. Howard, J. Johnson, K. X. Whipple, W. E. Dietrich, and J. T. Perron (2006), Can springs cut canyons into rock?, *J. Geophys. Res.*, *111*, E07002, doi:10.1029/2005JE002663.
- Lamb, M., W. E. Dietrich, and J. G. Venditti (2008), Is the critical Shields stress for incipient sediment dependent on channel-bed slope?, *J. Geophys. Res.*, *113*, F02008, doi:10.1029/2007JF000831.
- Lave, J., and J. P. Avouac (2001), Fluvial incision and tectonic uplift across the Himalayas of central Nepal, *J. Geophys. Res.*, *106*, 26,561–26,591, doi:10.1029/2001JB000359.
- Leopold, L. B. (1970), An improved method for size distribution of streambed gravel, *Water Resour. Res.*, *6*, 1357–1366, doi:10.1029/WR006i005p01357.
- Mackin, J. H. (1948), Concept of the graded river, *Geol. Soc. Am. Bull.*, *101*, 1373–1388.
- Marchetti, D. W., and T. E. Cerling (2001), Bedrock incision rates for the Fremont River: Tributary of the Colorado River, in *Colorado River Origin and Evolution: Proceedings of a Symposium Held at Grand Canyon National Park in June, 2000*, Grand Canyon Assoc. Monogr., vol. 12, edited by R. A. Young and E. E. Spammer, pp. 125–127, Grand Canyon Assoc., Grand Canyon, Ariz.
- Montgomery, D. R., and J. M. Buffington (1997), Channel-reach morphology in mountain drainage basins, *Geol. Soc. Am. Bull.*, *109*, 596–611, doi:10.1130/0016-7606(1997)109<0596:CRMIMD>2.3.CO;2.
- Montgomery, D. R., T. B. Abbe, N. P. Peterson, J. M. Buffington, K. M. Schmidt, and J. D. Stock (1996), Distribution of bedrock and alluvial channels in forested mountain drainage basins, *Nature*, *381*, 587–589, doi:10.1038/381587a0.
- Ouimet, W. B., K. X. Whipple, B. T. Crosby, J. P. Johnson, and T. F. Schildgen (2008), Epigenetic gorges in fluvial landscapes, *Earth Surf. Processes Landforms*, doi:10.1002/esp.1650.
- Parker, G., and C. M. Toro-Escobar (2002), Equal mobility of gravel in streams: The remains of the day, *Water Resour. Res.*, *38*(11), 1264, doi:10.1029/2001WR000669.
- Playfair, J. (1802), *Illustrations of the Huttonian Theory of the Earth*, Dover, London.
- Reid, I., J. B. Laronne, and D. M. Powell (1998), Flash-flood and bedload dynamics of desert gravel-bed streams, *Hydrol. Processes*, *12*, 543–557, doi:10.1002/(SICI)1099-1085(19980330)12:4<543::AID-HYP593>3.0.CO;2-C.
- Schumm, S. A., and R. J. Chorley (1966), Talus weathering and scarp recession in the Colorado plateaus, *Z. Geomorphol.*, *10*, 11–36.
- Seidl, M. A., and W. E. Dietrich (1992), The problem of channel erosion into bedrock, *Catena Suppl.*, *23*, 101–124.
- Sklar, L., and W. E. Dietrich (1998), River longitudinal profiles and bedrock incision models: Stream power and the influence of sediment supply, in *Rivers Over Rock: Fluvial Processes in Bedrock Channels*, *Geophys. Monogr. Ser.*, vol. 107, edited by K. J. Tinkler and E. E. Wohl, pp. 237–260, AGU, Washington, D. C.
- Sklar, L. S., and W. E. Dietrich (2001), Sediment and rock strength controls on river incision into bedrock, *Geology*, *29*(12), 1087–1090, doi:10.1130/0091-7613(2001)029<1087:SARSCO>2.0.CO;2.
- Sklar, L. S., and W. E. Dietrich (2004), A mechanistic model for river incision into bedrock by saltating bed load, *Water Resour. Res.*, *40*, W06301, doi:10.1029/2003WR002496.
- Sklar, L. S., and W. E. Dietrich (2006), The role of sediment in controlling steady-state bedrock channel slope: Implications of the saltation-abrasion incision model, *Geomorphology*, *82*, 58–83, doi:10.1016/j.geomorph.2005.08.019.
- Snyder, N. P., K. X. Whipple, G. E. Tucker, and D. J. Merritts (2003), Importance of a stochastic distribution of floods and erosion thresholds in the bedrock river incision problem, *J. Geophys. Res.*, *108*(B2), 2117, doi:10.1029/2001JB001655.
- Stock, J. D., and D. R. Montgomery (1999), Geologic constraints on bedrock river incision using the stream power law, *J. Geophys. Res.*, *104*, 4983–4993, doi:10.1029/98JB02139.
- Tomkin, J. H., M. T. Brandon, F. J. Pazzaglia, J. R. Barbour, and S. D. Willett (2003), Quantitative testing of bedrock incision models for the Clearwater River, NW Washington State, *J. Geophys. Res.*, *108*(B6), 2308, doi:10.1029/2001JB000862.
- Tucker, G. E., and R. L. Slingerland (1994), Erosional dynamics, flexural isostasy, and long-lived escarpments: A numerical modeling study, *J. Geophys. Res.*, *99*, 12,229–12,243, doi:10.1029/94JB00320.
- Turowski, J. M., N. Hovius, H. Meng-Long, D. Lague, and C. Men-Chiang (2007a), Distribution of erosion across bedrock channels, *Earth Surf. Process Landforms*, *33*, 353–363, doi:10.1002/esp.1559.
- Turowski, J. M., N. Hovius, A. Wilson, and M.-J. Horng (2007b), Hydraulic geometry, river sediment and the definition of bedrock channels, *Geomorphology*, *99*, 26–38, doi:10.1016/j.geomorph.2007.10.001.
- Turowski, J. M., D. Lague, and N. Hovius (2007c), Cover effect in bedrock abrasion: A new derivation and its implications for the modeling of bedrock channel morphology, *J. Geophys. Res.*, *112*, F04006, doi:10.1029/2006JF000697.
- van der Beek, P., and P. Bishop (2003), Cenozoic river profile development in the Upper Lachlan catchment (SE Australia) as a test of quantitative fluvial incision models, *J. Geophys. Res.*, *108*(B6), 2309, doi:10.1029/2002JB002125.
- Vutukuri, V. S., R. D. Lama, and S. S. Saluja (1974), *Handbook on Mechanical Properties of Rocks*, vol. 1, *Testing Techniques and Results*, 280 pp., Trans Tech., Bay Village, Ohio.
- Whipple, K. X. (2004), Bedrock rivers and the geomorphology of active orogens, *Annu. Rev. Earth Planet. Sci.*, *32*, 151–185, doi:10.1146/annurev.earth.32.101802.120356.
- Whipple, K. X., and G. E. Tucker (1999), Dynamics of the stream-power river incision model: Implications for height limits of mountain ranges, landscape response time scales, and research needs, *J. Geophys. Res.*, *104*, 17,661–17,674, doi:10.1029/1999JB900120.
- Whipple, K. X., and G. E. Tucker (2002), Implications of sediment-flux-dependent river incision models for landscape evolution, *J. Geophys. Res.*, *107*(B2), 2039, doi:10.1029/2000JB000044.
- Wilcock, P. R., and J. C. Crowe (2003), Surface-based transport model for mixed-size sediment, *J. Hydraul. Eng.*, *129*, 120–128, doi:10.1061/(ASCE)0733-9429(2003)129:2(120).
- Willgoose, G., R. L. Bras, and I. Rodriguez-Iturbe (1991), A coupled channel network growth and hillslope evolution model: 1. Theory, *Water Resour. Res.*, *27*, 1671–1684, doi:10.1029/91WR00935.
- Wobus, C., K. X. Whipple, E. Kirby, N. Snyder, J. P. Johnson, K. Spyropolou, B. Crosby, and D. Sheehan (2006), Tectonics from topography: Procedures, promise and pitfalls, in *Tectonics, Climate, and Landscape Evolution*, edited by S. D. Willett et al., *Spec. Pap. Geol. Soc. Am.*, *398*, 55–74, doi:10.1130/2006.2398(04).
- Wohl, E. E., D. J. Anthony, S. W. Madsen, and D. M. Thompson (1996), A comparison of surface sampling methods for coarse fluvial sediments, *Water Resour. Res.*, *32*, 3219–3226, doi:10.1029/96WR01527.
- Yager, E. M., J. W. Kirchner, and W. E. Dietrich (2007), Calculating bed load transport in steep boulder bed channels, *Water Resour. Res.*, *43*, W07418, doi:10.1029/2006WR005432.
- Zimmermann, A., and M. Church (2001), Channel morphology, gradient profiles and bed stresses during flood in a step-pool channel, *Geomorphology*, *40*, 311–327, doi:10.1016/S0169-555X(01)00057-5.

T. C. Hanks, U.S. Geological Survey, 345 Middlefield Road, Menlo Park, CA 94025, USA.

J. P. L. Johnson, Jackson School of Geosciences, University of Texas at Austin, Austin, TX 78712, USA. (joelj@jsg.utexas.edu)

L. S. Sklar, Department of Geosciences, San Francisco State University, San Francisco, CA 94132, USA.

K. X. Whipple, School of Earth and Space Exploration, Arizona State University, Tempe, AZ 85287, USA.